AD-A083 230 UNITED TECHNOLOGIES RESEARCH CENTER EAST HARTFORD CONN F/G 20/5
NOVEL RESONATORS FOR HIGH POWER CHEMICAL LASERS,(U)
1979 H R GARCIA, G E PALMA, A W ANGELBECK N00173-79-C-0410
UNCLASSIFIED NL

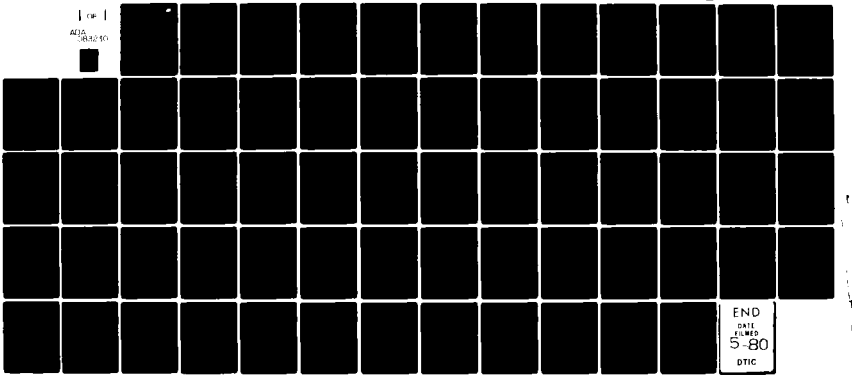

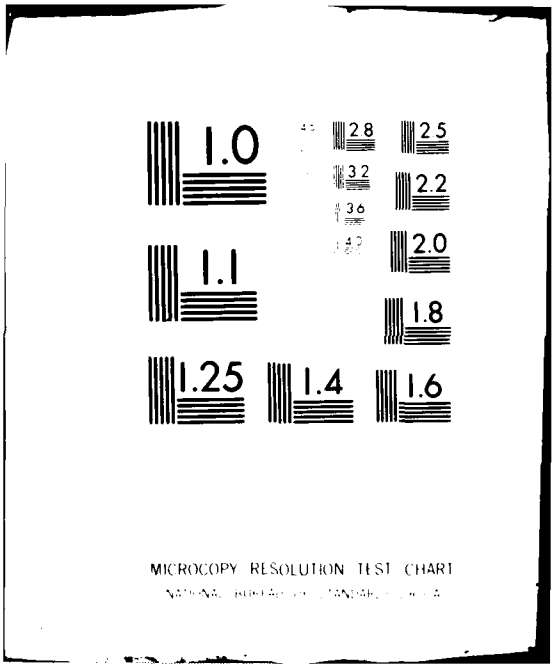
1.0
2.8
2.5
3.2
2.2
3.6
2.0
1.1
1.8
1.25
1.4
1.6
MICROCOPY RESOLUTION TEST CHART

LEVEL II

12

NOVEL RESONATORS FOR HIGH POWER CHEMICAL LASERS

Letter
Final Report

Contract N00173-79-C-0410

Authors: H.R. Garcia, G.E. Palma, A.W. Angelbeck of
United Technologies Research Center and
R.D. Quinnell, J.B. Urquhart of P&WA
Government Products Division

Prepared for

Naval Research Laboratory
Washington, D.C. 20375

NOVEL RESONATORS FOR HIGH POWER CHEMICAL LASERS

LETTER FINAL REPORT

CONTRACT N00173-79-C-0410

AUTHORS: H.R. GARCIA, G.E. PALMA, A.W. ANGELBECK OF UNITED TECHNOLOGIES RESEARCH CENTER AND R.D. QUINNELL, J.B. URQUHART OF P&WA GOVERNMENT PRODUCTS DIVISION

PREPARED FOR

NAVAL RESEARCH LABORATORY

WASHINGTON, D.C. 20375

TABLE OF CONTENTS

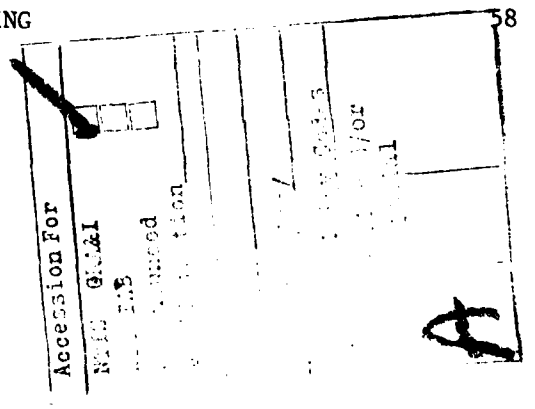

LIST OF ILLUSTRATIONS

1. INTRODUCTION

The Novel Resonator Program resulted from a growing interest in radial-flow, high power chemical lasers. Because of this interest, a great deal of attention has been focused upon developing resonator geometries which are capable of efficiently extracting energy from the thin cylindrical sheath of active medium generated by the radial flow nozzle array. Of particular importance is that the extracted power be characterized by near diffraction-limited beam quality. Additional characteristics must also be considered such as sensitivity to misalignment, susceptibility to parasitics, mode medium effects, practicability of multiwavelength operation, manufacturability of the optical components, and scalability to high power.

Over the past several years, a number of annular resonator concepts have emerged that offer high power potential. Three such resonators that were conceived during the ALOS program are HSURIA, Ring HSURIA, and the converging wave resonator. The single axis resonator for annular devices (SARAD), as well as the unstable resonator with self-imaging apertures, are configurations which have more recently been conceived by AFWL. The ring resonator with intracavity focal line aperture (IFLA) is a promising annular resonator concept presently being investigated by UTC. U.T.R.C. has also investigated various injection locking schemes, multiple resonator phased array, and master oscillator power amplifier (MOPA) configurations for annular device applications.

By drawing on the analysis of these concepts seven resonator categories were considered for the Novel Resonator Program. These were as follows:

1. Intracavity Spatial Filtering
2. Converging Wave Resonators
3. Self Imaging Resonators
4. Injection Locking
5. MOPA Configuration
6. Diffractive Cross Coupling
7. Multiple Beam Resonator Concept.

Based on investigations done by P&WA and U.T.R.C., injection locking was decided to be the most promising candidate. With the concurrence of NRL/DARPA, this concept was selected for further study.

The primary advantage of injection locking is the enhanced mode discrimination. Theoretically, the frequency, phase, and mode properties of the high power annular resonator are determined by the nature of the laser beam which is injected into the annular resonator from a low-power, frequency-stable, mode selective master oscillator.

2. ANALYSIS AND RESULTS

2.1 Baseline Configuration Definition

The baseline configuration, shown in Figure 1, is a confocal asymmetric ring resonator with a pair of W-axicons for beam compacting and an axial injection coupling hole in the feedback portion of the ring. Most of the effort in this investigation has been devoted to injection locked operation in which the undriven ring is capable of self-oscillation. This regime offers better power extraction than the regenerative amplification regime, but is also more problematic due to stringent cavity length matching requirements and the need to suppress backward wave oscillation.

The geometric analysis of the configuration shown in Figure 1 and its compacted equivalent, shown in Figure 2, are detailed in Appendix A. The objectives of this analysis are to provide a range of parameters for the code calculations. In particular, expressions were derived relating the required injected power and the phase locking range for injection control to the resonator cavity magnification M, and the diameter of the injection coupler, D_2.

Figure 3 shows the variation of required injected power, P_o, normalized to the self-oscillation power of the ring, P_{osc}, with the ratio of the inner diameter of the output coupler, D_c, to the diameter of the injected coupling hole, D_2. These curves indicate that for

$$P_o/P_{osc} < .01$$

$$m = D_c/D_2 > 5 \text{ for } M=2$$

$$m > 3 \text{ for } M=3.$$

The maximum value of $D_2 = D_c/m$ is, thus, set by the abailable MO power. The minimum value of D_2 is established by the phase locking range, δ_1. If δ_1 is too small, it will be difficult to match the cavity length of MO and ring to the desired accuracy for efficient power extraction. The relationship between δ_1 and the

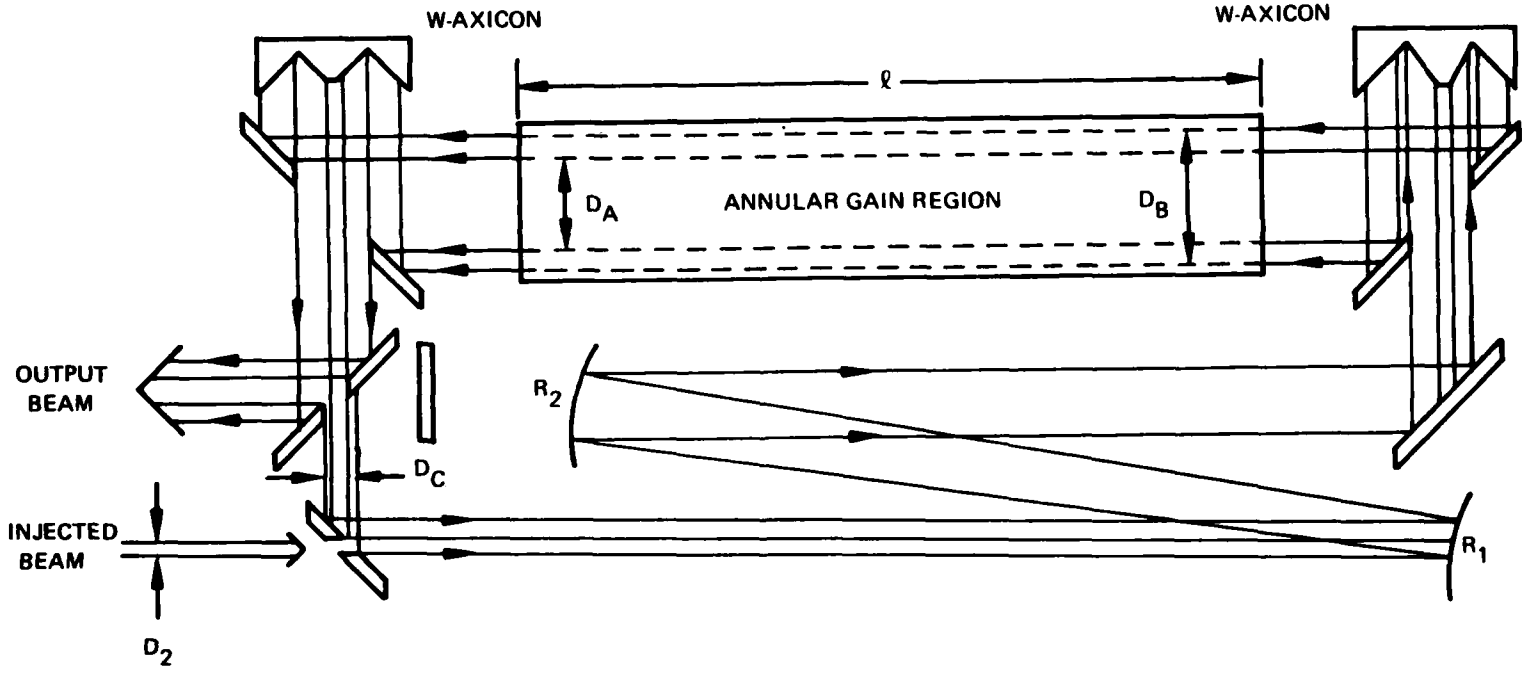

Figure 1. Injection Controlled Annular Ring

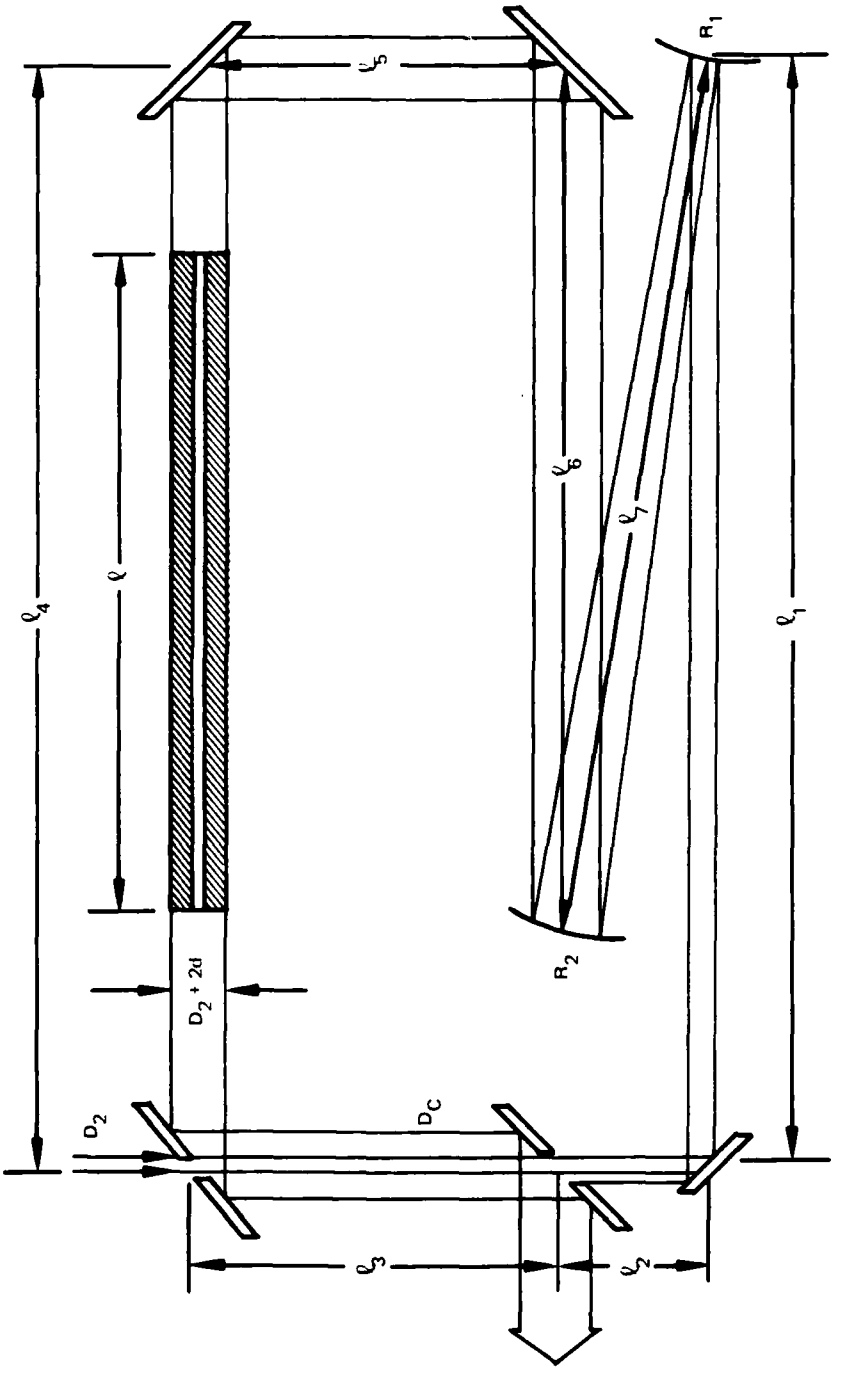

Figure 2. Compacted Equivalent Asymmetric Ring

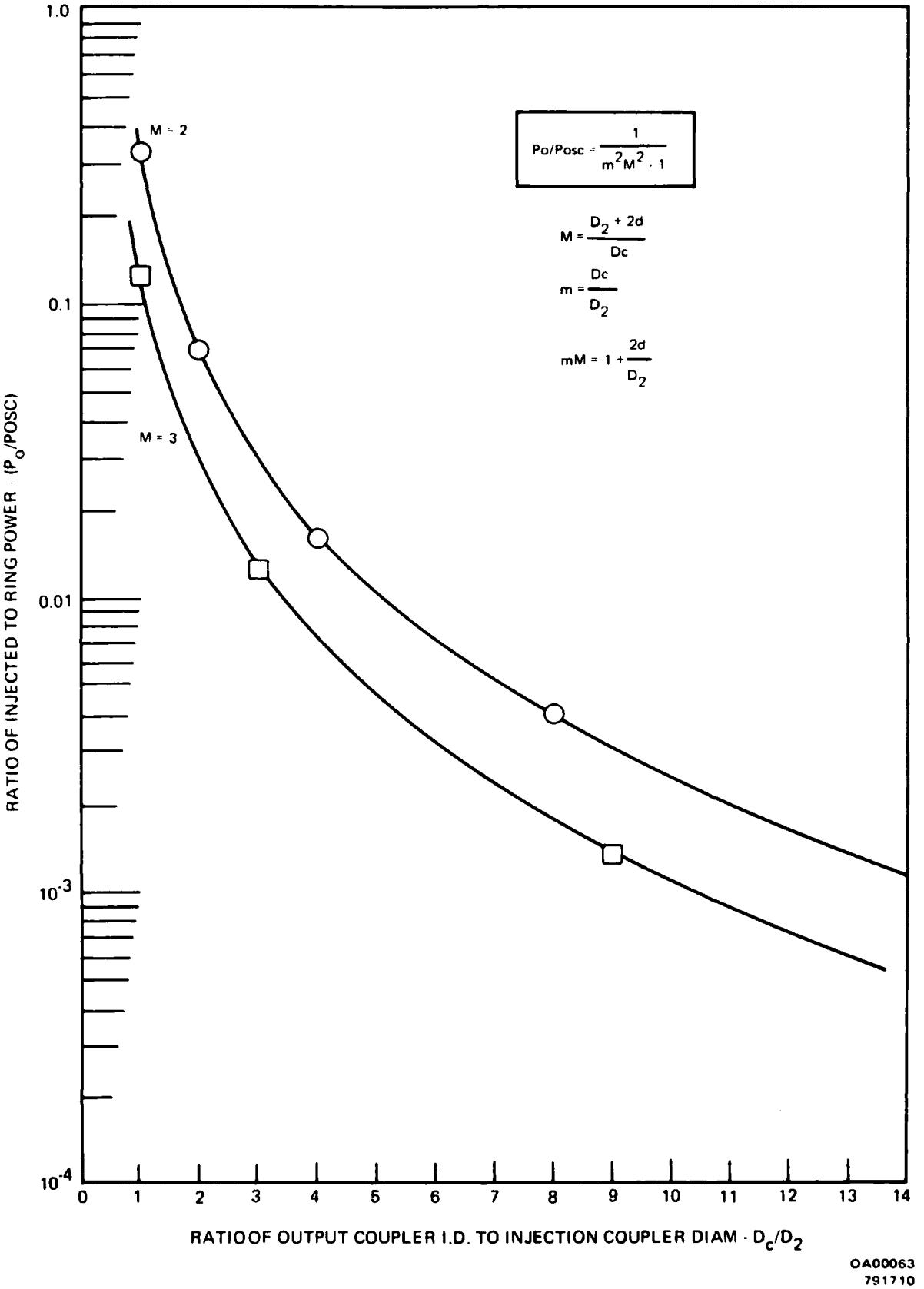

Figure 3. Injection Power Requirement

resonator parameters, m and M, is given by equation 14 derived in Appendix A:

$$\delta_1 = \sqrt{\frac{M^2 - 1}{m^2M^2 - 1}} \qquad (1)$$

or approximately,

$$\delta_1 \simeq 1/m$$

A reasonable value for closed loop phase error is $\delta = 0.1$ rad, which gives a maximum value of $m = 10$. Thus, this analysis indicates a range of interest of,

$$3 < m < 10, \text{ where } m = D_c/D_2$$

and from Figure 3 $\quad 10^{-3} < P_o/P_{osc} < 10^{-2}$

with $\quad 0.1\ \delta_1 < 0.35$ rad.

2.2 Optical Analysis - Compacted Ring Resonator

The initial optical analysis was done on the bare compacted equivalent of the baseline configuration (see Figure 2). This approach was taken because the rectangular SOQ Computer code was available and the annular code was still under development.

Table 1 lists the physical characteristics of the resonator used for initial analysis. This resonator was converged without an injection signal, and the mode structure recorded at the location to be used for injection. The resonator was then re-converged using the recorded mode structure as an injected signal. Figure 4 shows the intensity distribution of the field incident on the hole coupler without injection. The results with injection are identical.

To investigate the effect of injection on the compacted equivalent ring resonator, misalignment and astigmatism sensitivity studies were performed. The results of the misalignment study are summarized in Figures 5 and 6. The baseline and injected resonators were modeled with various levels of misalignment (tilt) applied at an optic approximately half-way around the ring from the hole coupler. Figure 5 shows the effect of tilt on bare resonator power coupling to be negligible

TABLE 1 PHYSICAL CHARACTERISTICS OF ANALYTICAL DESIGN

Wavelength (single line)	3.8 microns
Magnification	3.0
Convex Mirror Radius of Curvature	100 cm
Concave Mirror Radius of Curvature	300 cm
Geometric Beam Diameter	10 cm
Injected Beam Diameter	1.11 cm
Resonator Length	1460 cm
Equivalent Fresnel Number	4.5
Collimated Fresnel Number	10.1
Mirror Reflectivity	0.99
Mirror Distortion	None

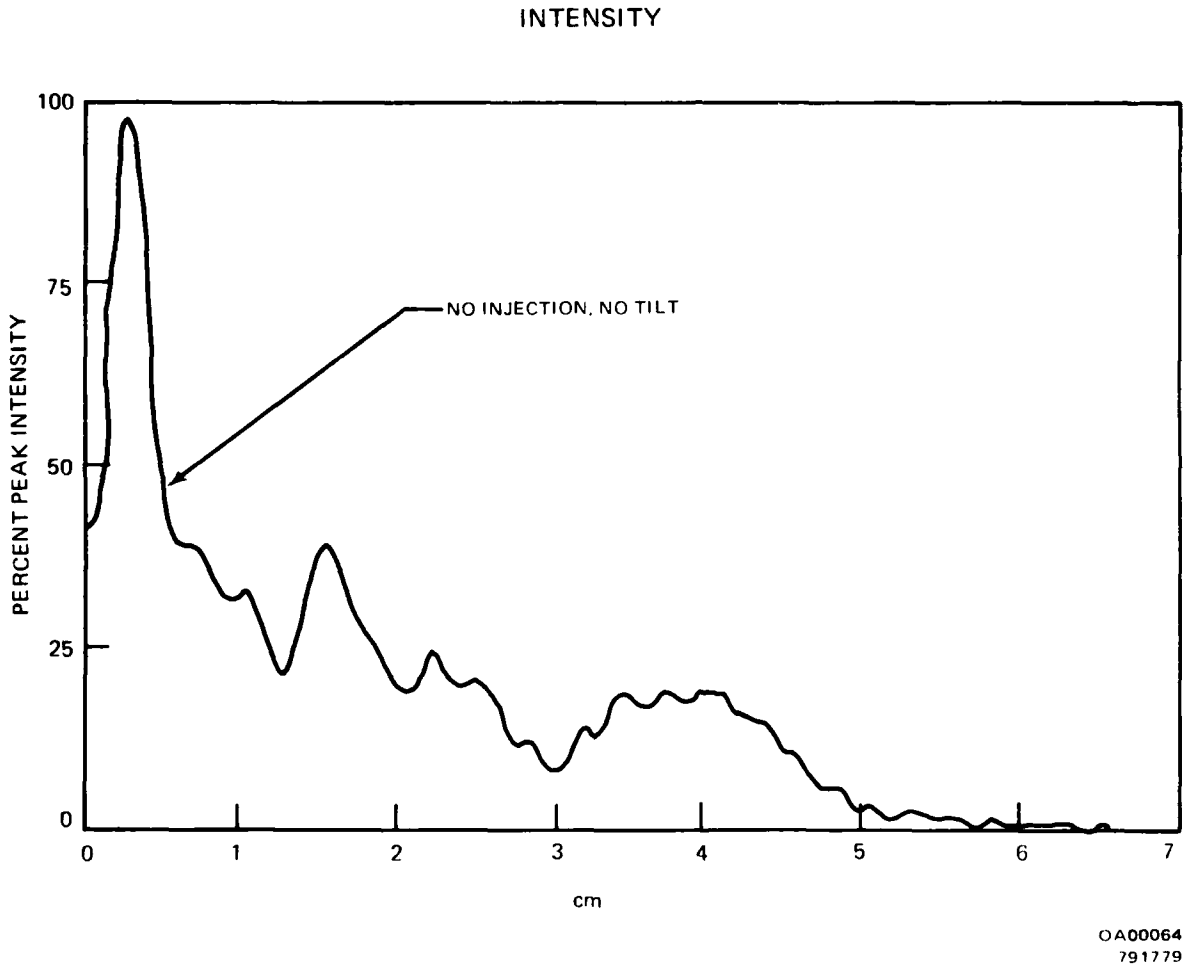

Figure 4. Preliminary Bare Resonator Results

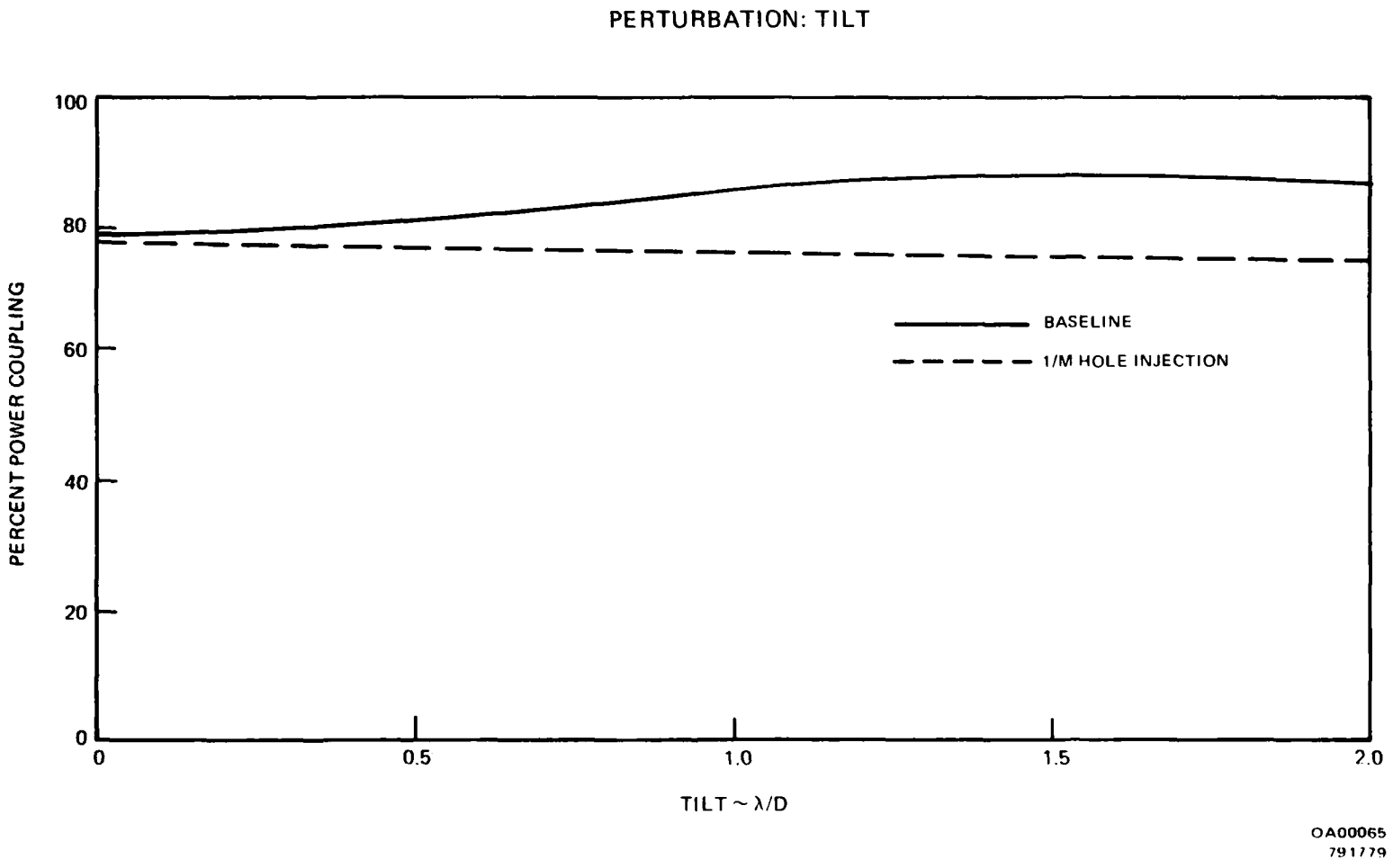

Figure 5. Injection Locking Effect On Power Coupling

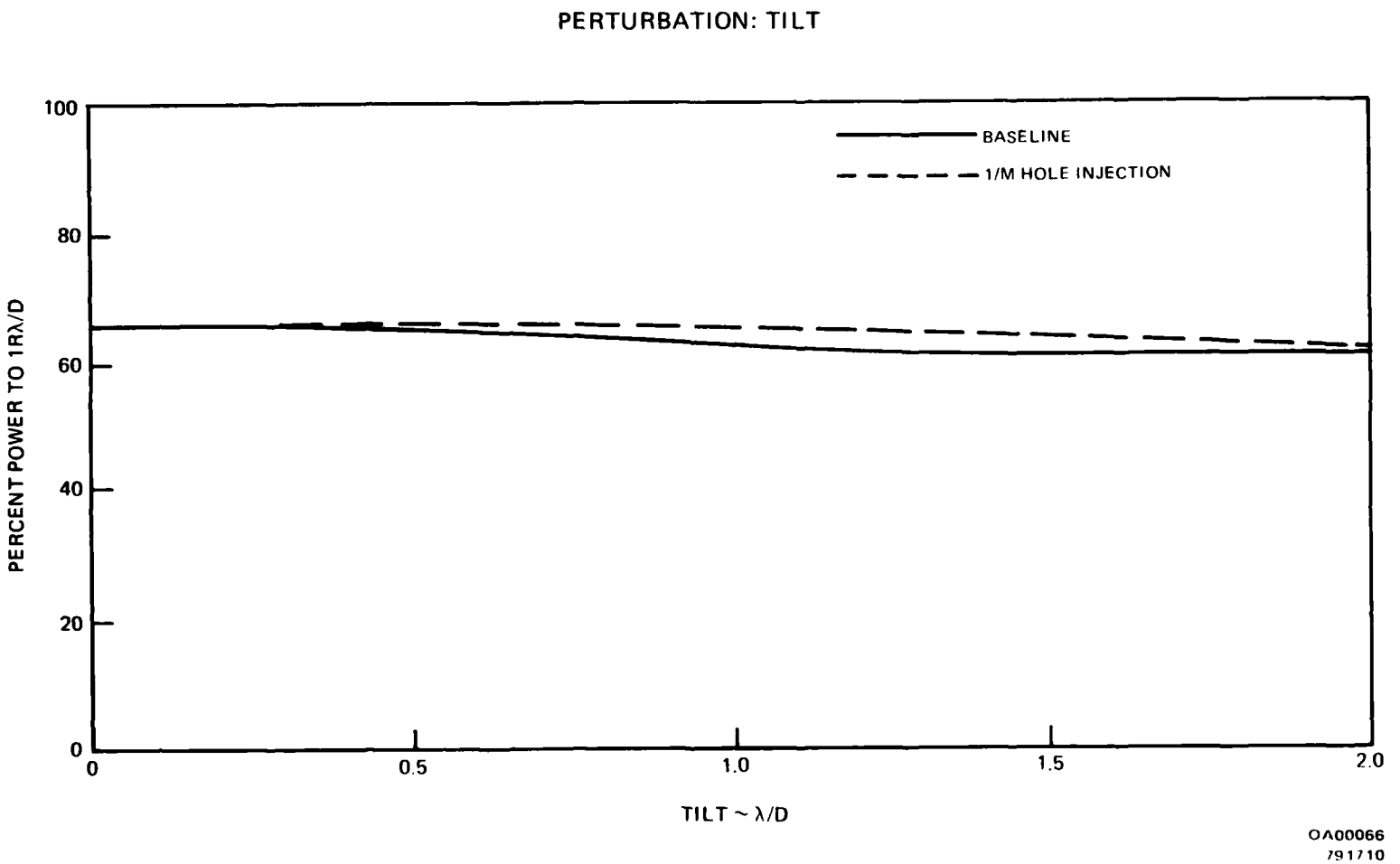

Figure 6. Injection Locking Effect On Beam Quality

for the injected case. A slight improvement in beam quality (Figure 6) is possible for misalignment up to $2\ell/D$. Beyond this level, quality degradation becomes worse for the injected case.

Figures 7, 8, and 9 summarize the results of an astigmatism sensitivity study. During this study, several methods and levels of injection were modelled: A single on-axis injection beam coupled into the field with a hole coupler 1/M times the feedback beam diameter, a grating (or splitter) coupling in an injection beam the size and power of the feedback beam, and a lower power version of the grating injector scheme. Figure 7 indicates that power coupling can be held constant for various levels of astigmatism. The value of power coupling is set by the specific injection technique. As shown in Figures 8 and 9, no appreciable gain or loss in beam quality is attributable to any of the injection methods.

The addition of a simple uniform saturable gain in one leg of the resonator was not informative. Resonator results were essentially identical for the baseline, perturbed (astigmatism), and perturbed-with-injection cases.

In addition to these sensitivity studies, a vertical obscuration or strut was added to the compact ring configuration to force the resonator to run with a two-lobed mode structure. The presence of a strut significantly reduced output beam quality and increased power coupling to nearly 97 percent. An optical "kernel" from the baseline (no strut) resonator was injected in the geometric shadow of the strut. The injected resonator showed a significant improvement in beam quality and power coupling but did not return to values near the baseline case. This test represents the most improvement in resonator performance due to injection control observed in the compacted ring resonator.

The rate of improvement in power coupling and beam quality with injection signal strength is shown in Figure 10. Full injection strength was taken to be the power associated with that portion of the baseline, non-injected resonator. Figure 10 indicates half the quality improvement available occurs at less than 15 percent of full injection power.

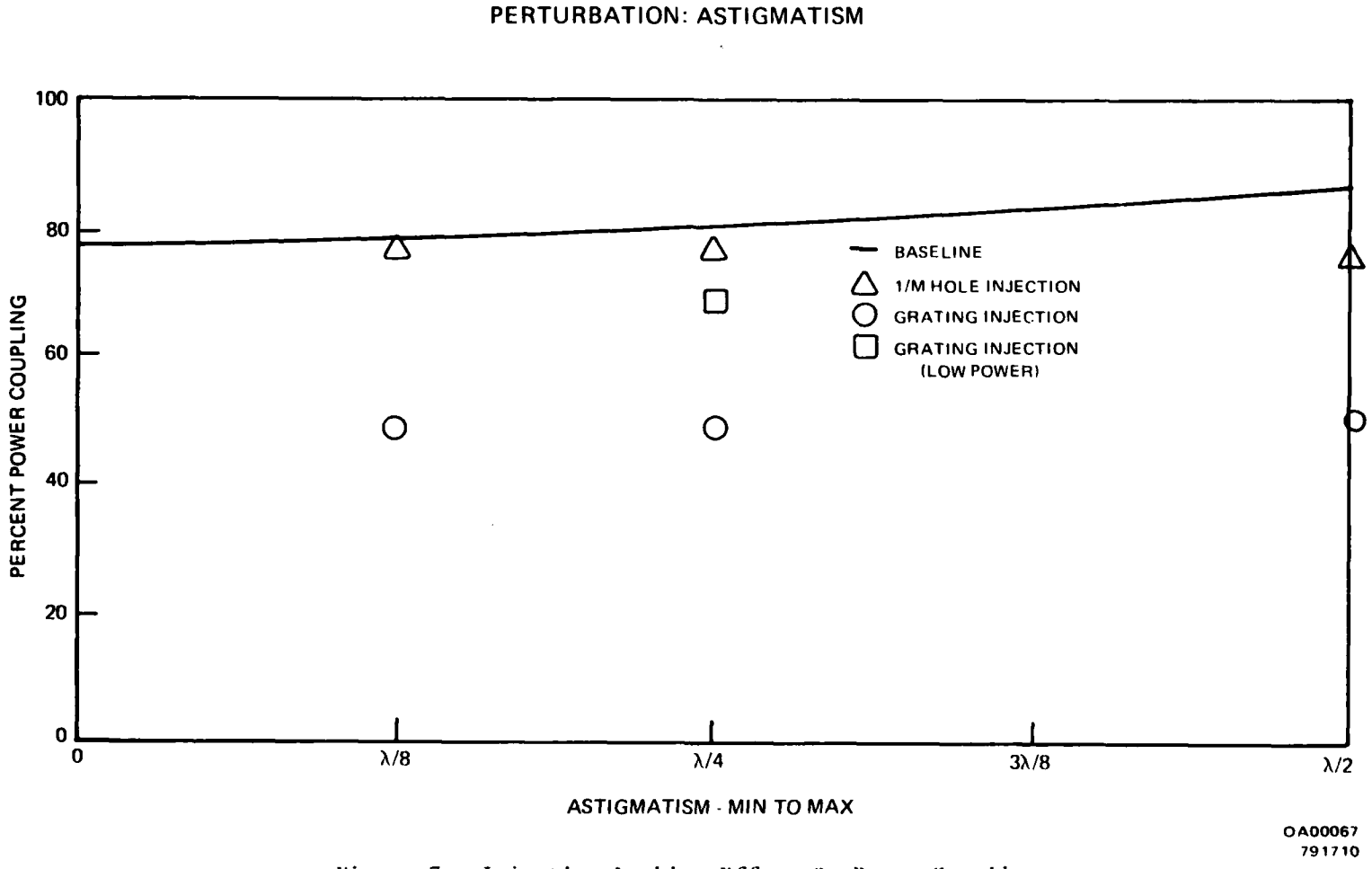

Figure 7. Injection Locking Effect On Power Coupling

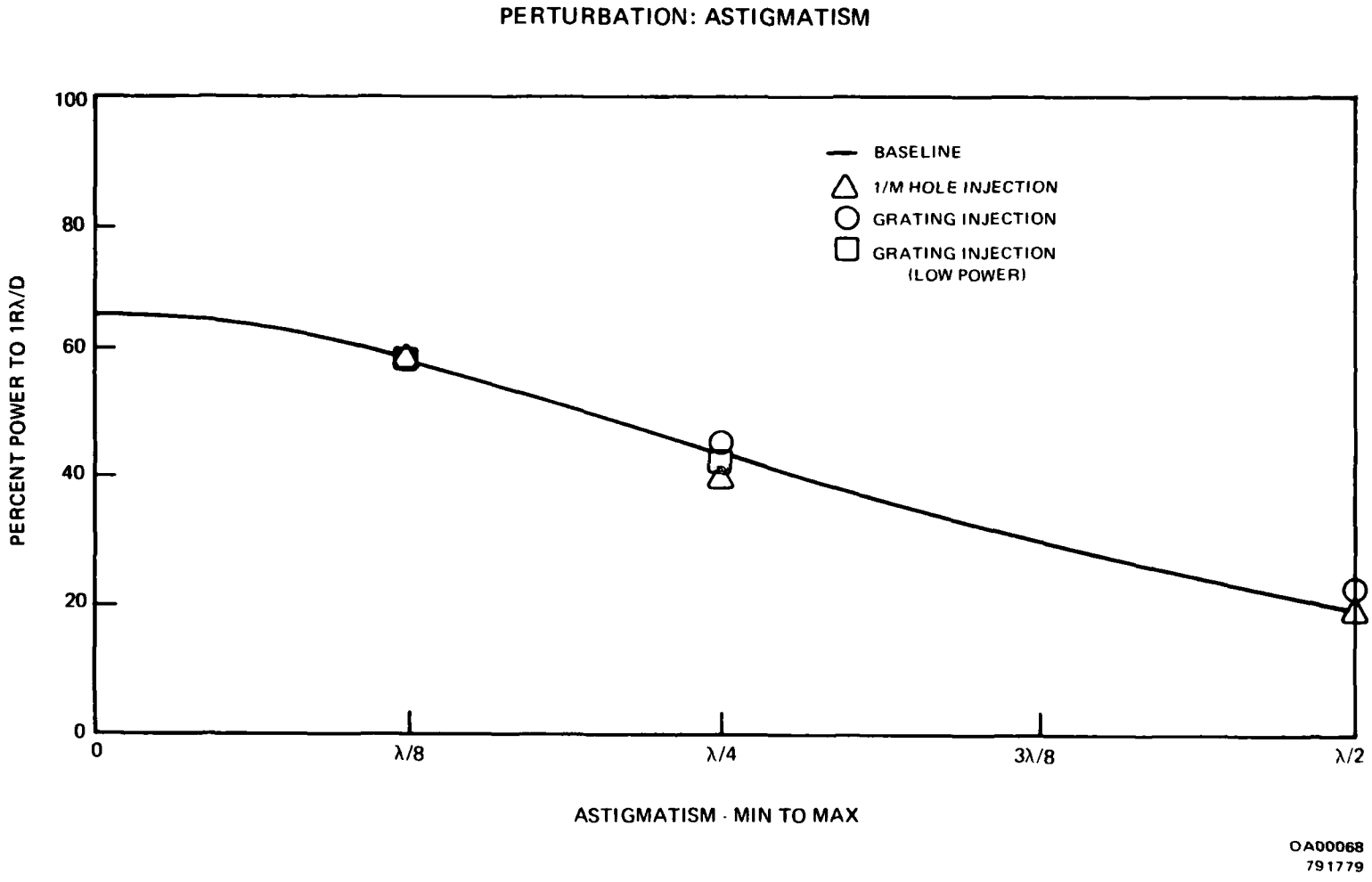

Figure 8. Injection Locking Effect On Beam Quality

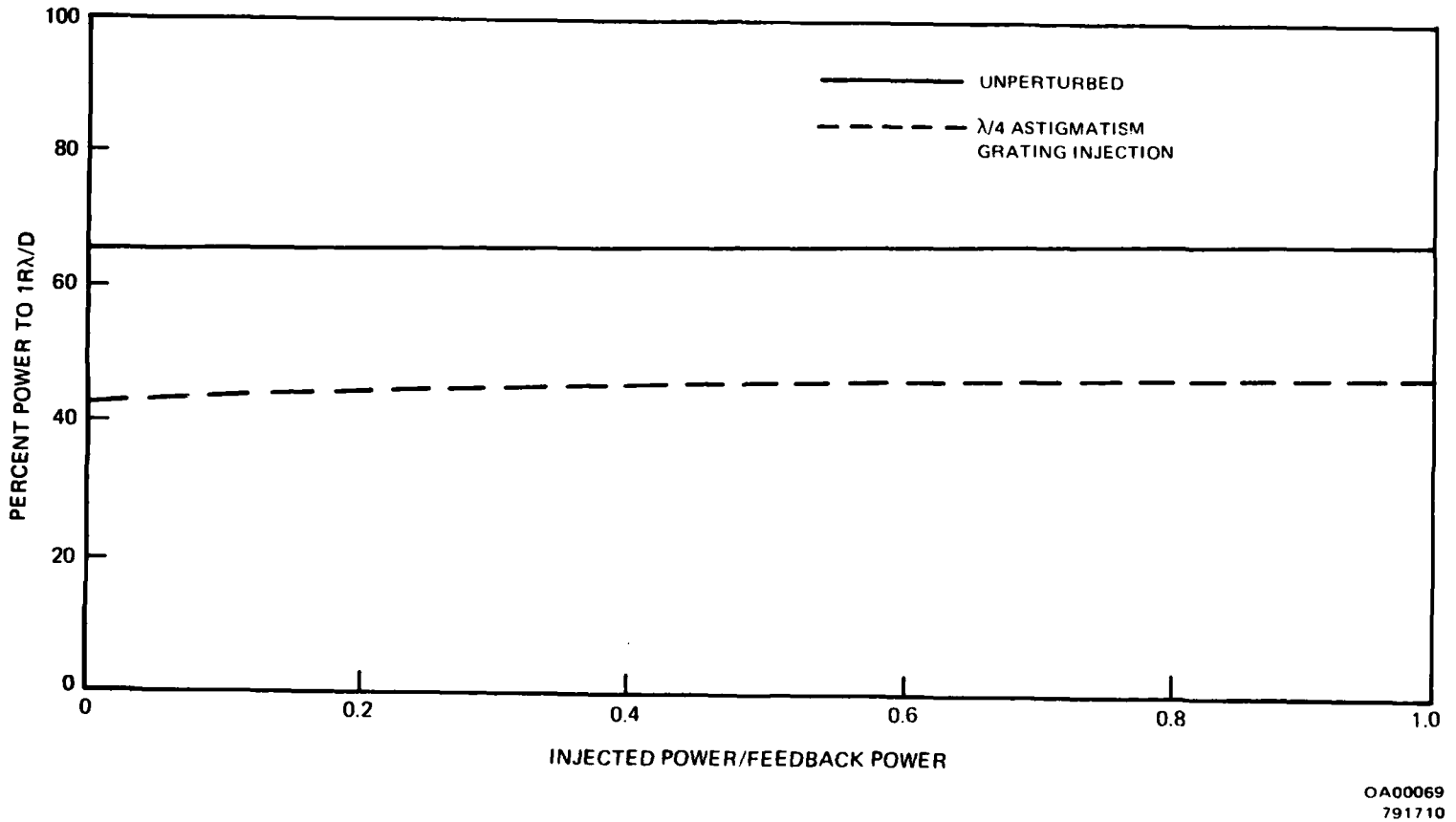

Figure 9. Injection Power Level Effect On Beam Quality

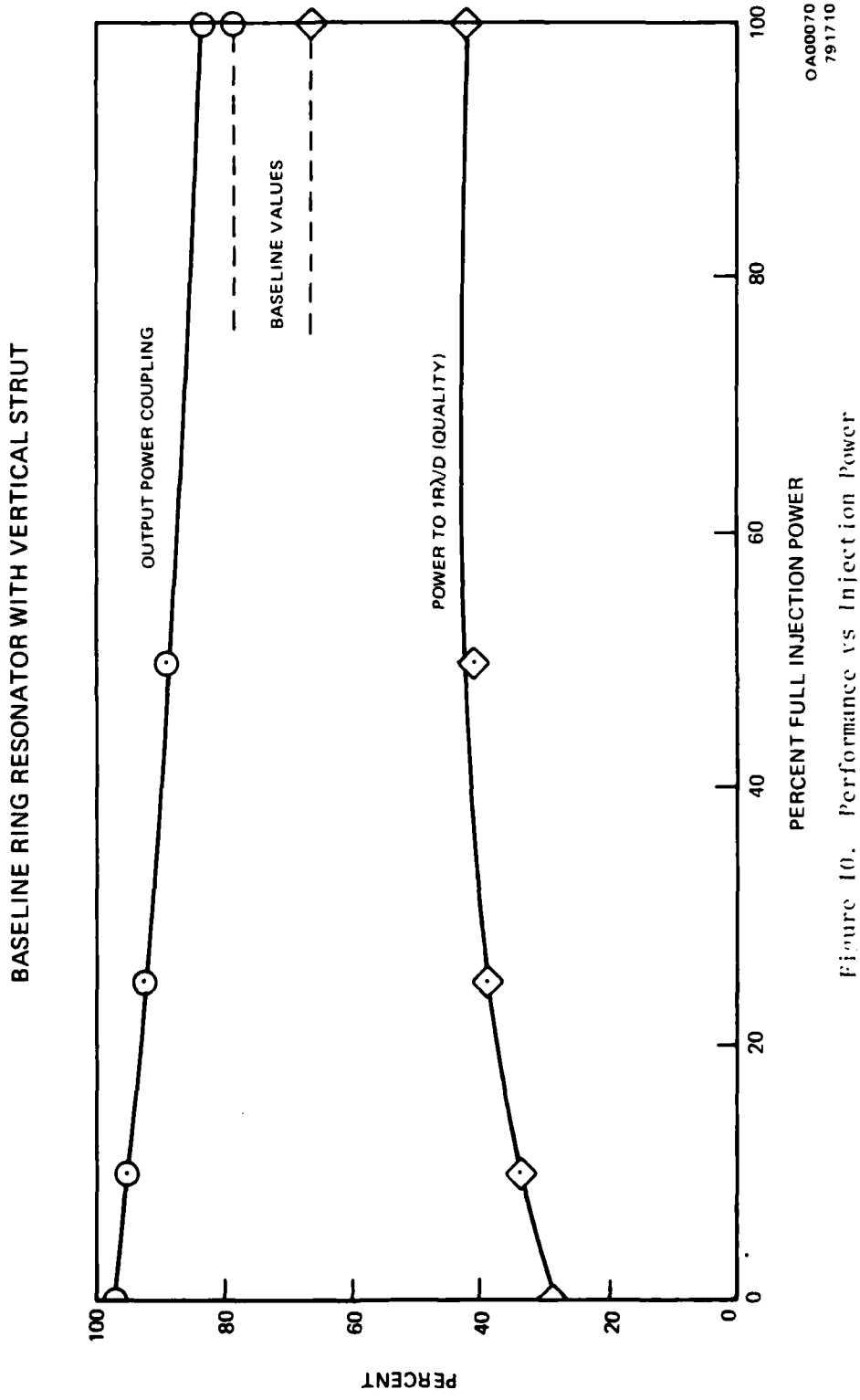

Figure 10. Performance vs Injection Power

A second resonator variation was run with various injection strengths. This resonator was altered to have an equivalent Fresnel number of 4.0, theoretically a poor design for mode discrimination. This resonator failed to converge without injection, but did settle to a single solution in the presence of the injection hole. Figure 11 indicates the rate of performance improvement with injection signal strength. Again, the injected signal was taken from the center of the baseline case with no struts and an equivalent Fresnel number of 4.5.

A review of these results for the equivalent compacted resonator indicates that injection can improve beam quality in some circumstances. However, improvement back to the unperturbed, aligned resonator results does not occur. Injection does, however, help maintain power coupling at the unperturbed value.

2.3 Optical Analysis - Annular Ring Resonator

The bare optical analysis was performed on the annular ring resonator shown in Figure 12. This configuration is essentially the same as that shown in Figure 1 with one exception. For comparison with the compacted resonator results, injection was moved to the compacting W-axicon.

Total path length and optical element separations were identical to the compact ring configuration used in previous analysis, thereby preserving the Fresnel number. The injection signal used in the annular resonator study was taken from the center of the unperturbed solution for the compact resonator. The annular resonator includes w-axicon tip truncation which precludes the use of nearaxial information for the unperturbed case.

The aligned annular resonator solution without injection resembles the compact solution with a hole on axis in terms of output power coupling. As expected, the mode structure draws away from the hole on axis (Figure 13). The introduction of an injection signal reduces power coupling and improves beam quality assemtially to the values for a compact resonator with no hole on axis (Figure 14.)

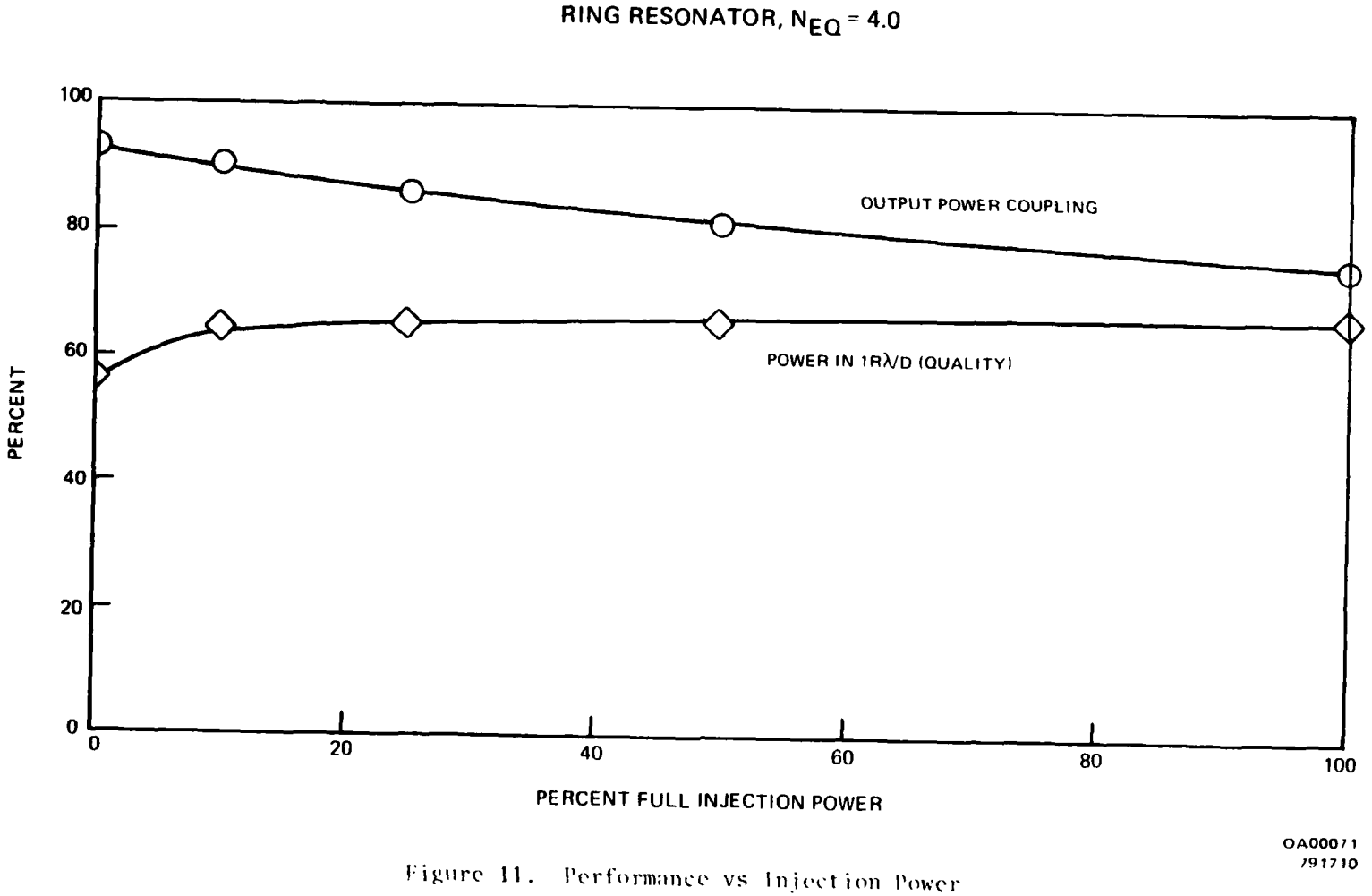

Figure 11. Performance vs Injection Power

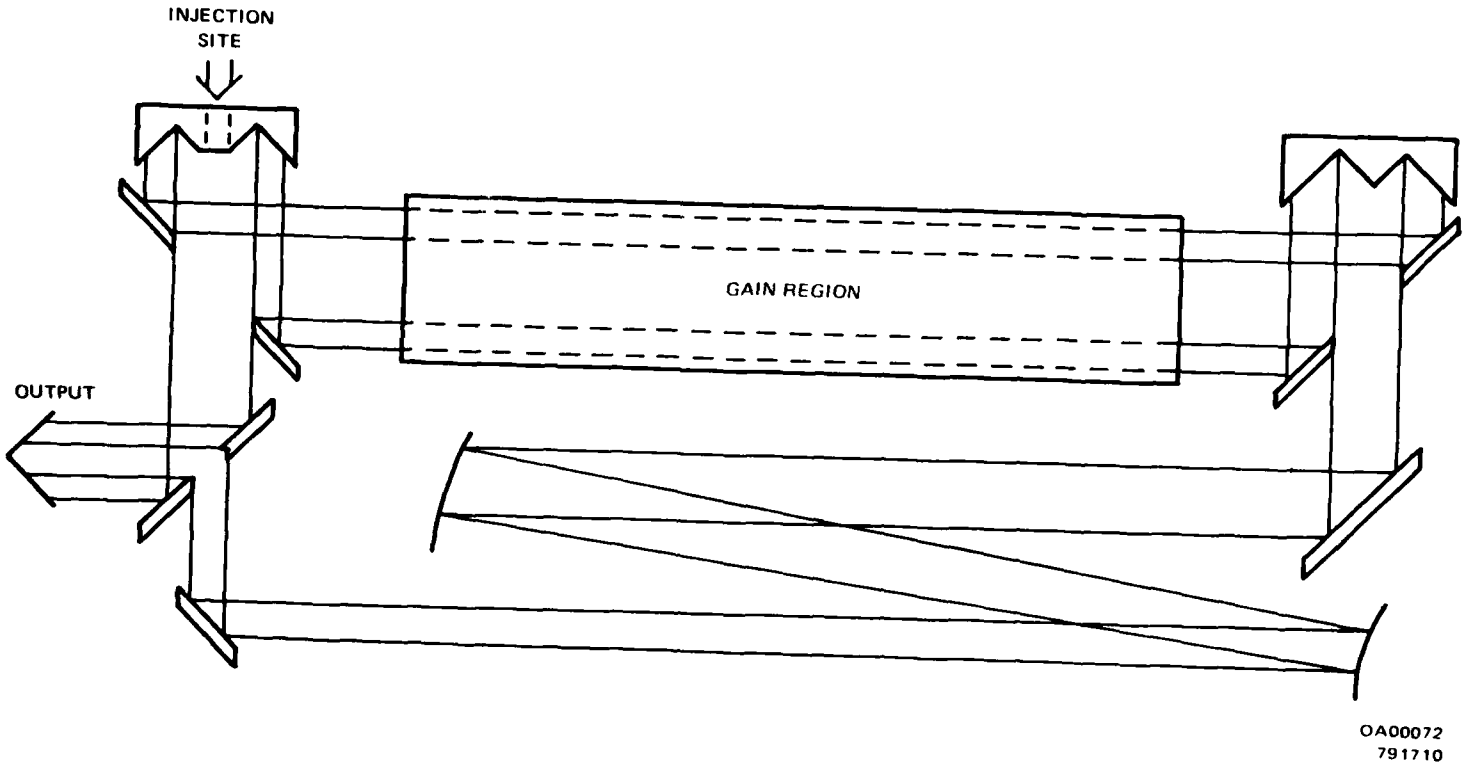

Figure 12. Annular Ring Resonator

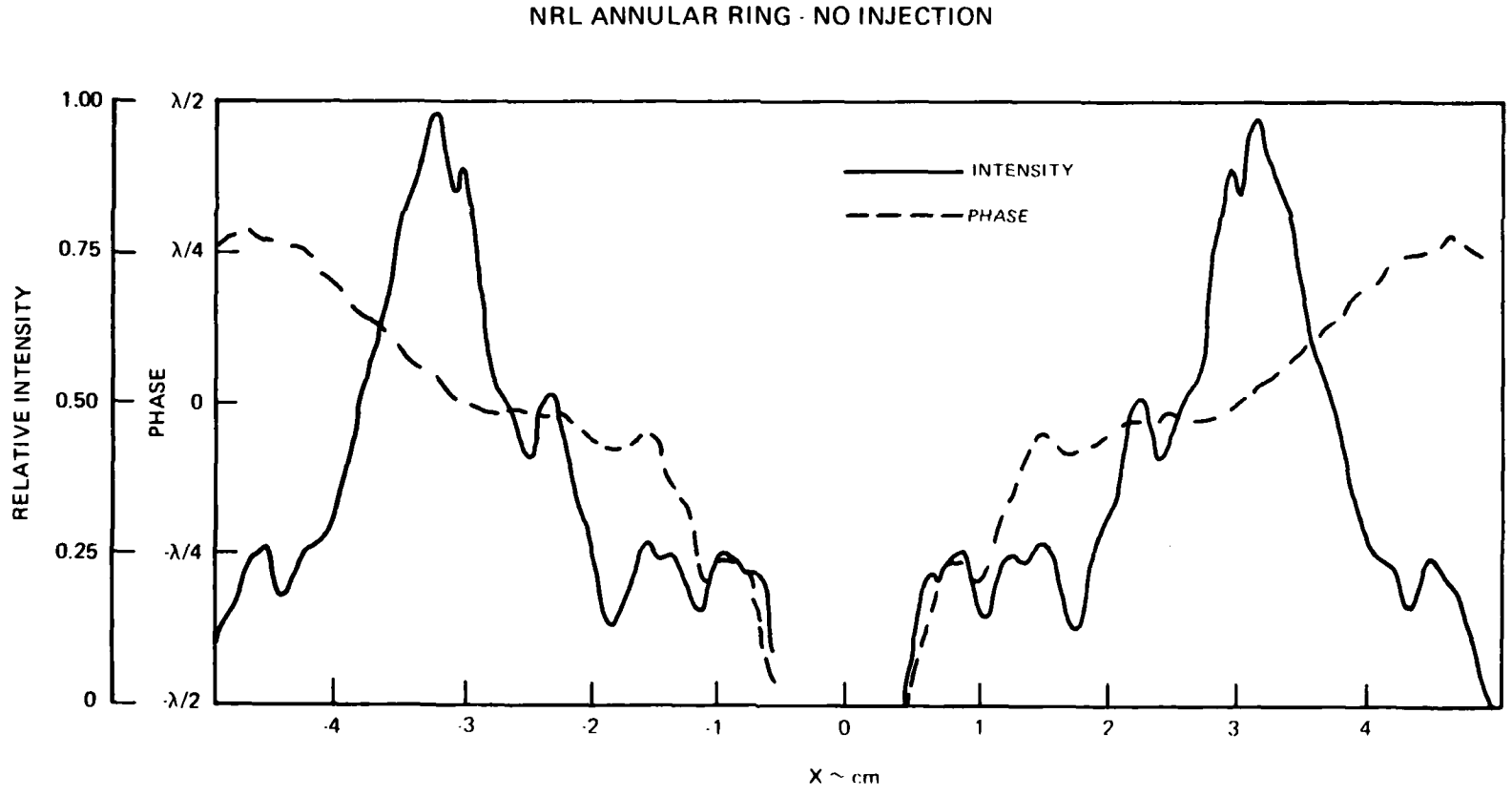

Figure 13. Field Incident On HCM

(20)

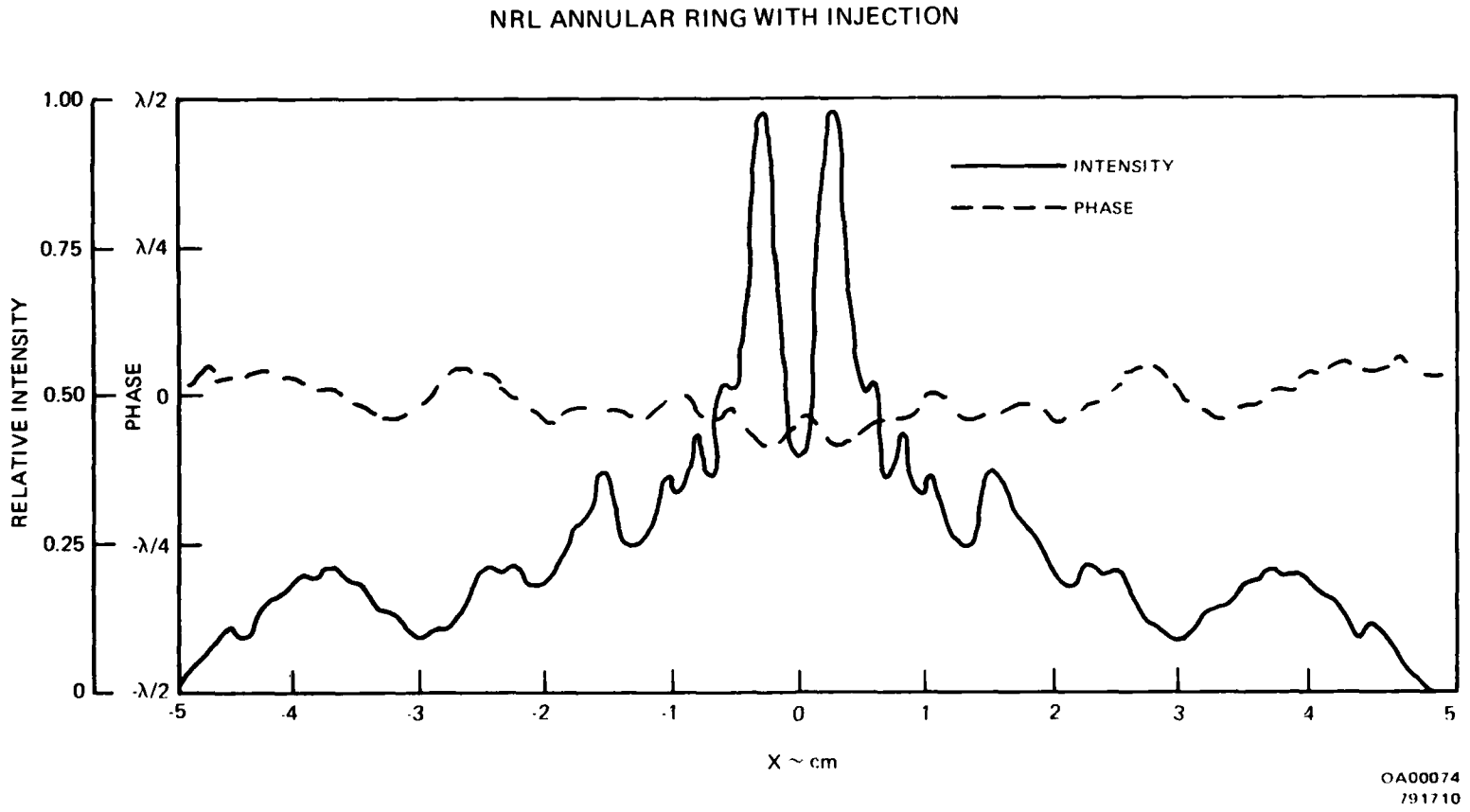

Figure 14. Field Incident On HCI

Table 2 compares power coupling and beam quality for the aligned compact and annular ring configurations. Two misaligned annular configurations are included. These cases demonstrate the most significant performance improvement due to injection control observed in the bare resonator analysis.

The history of misalignment cases leading to the two shown in Table 2 indicates a much higher sensitivity for the annular resonator as compared to the equivalent compact resonator. The computer model converged to a solution for the compact resonator with as much as 75 microradians mirror misalignment. The annular resonator would not converge with even 5 microradians of tilt unless it was injected with an unperturbed solution. The two cases listed in Table 2 have 1 and 2 microradians of tilt and show a significant degradation in beam quality for the non-injected cases.

Loaded resonator analysis began after modifications were made to the multi-wavelength code. The first resonator to be analyzed is the loaded equivalent to the baseline configuration with w-axicons to create the annular segment and no injected beam. The baseline case is necessarily first since it is the source of the injection signal used in other cases.

Operating the loaded resonator code has proved to be time-consuming. The code was still under development when loaded resonator analysis commenced. As a result, the baseline configuration without injection has been impacted by code corrections that were being made under the program responsible for developing the model. Faulty computer tapes, used to record information from iteration to iteration, has also contributed to delays. In spite of these problems, the baseline no-injection case has been run. The power in the 20 transitions selected were driven to zero in 12 iterations. This suggests that either the baseline configuration needs to be

TABLE 2. RING RESONATOR PERFORMANCE

	PERCENT OUTCOUPLING		PERCENT POWER TO 1 R λ/D	
	NON-INJECTED	INJECTED	NON-INJECTED	INJECTED
COMPACT, NO HOLE ON AXIS	78	77	66	67
COMPACT, HOLE ON AXIS	95	77	58	67
ANNULAR, ALIGNED	95	75	63	65
ANNULAR, 1 μ RADIAN TILT	93	75	45	65
ANNULAR, 2 μ RADIAN TILT	93	75	47	65

changed in some way so that less power is coupled out or that there is a problem in the code optics analysis, the kinetics package, or the integration of these two.

2.4 Analysis of Multiline Injection Locking

The multiline injection locking analysis detailed in Appendices B-D consists of (1) development of closed form expressions for saturated gain for multiline cascade coupled transitions, (2) development of a stable resonator equivalent of the injection controlled unstable ring, and (3) a perturbation analysis of the model to determine the form of the output power and phase angle in the case of multiline injection locking. The results are simple expressions for the phase locking range and cavity length matching requirements for coupled and uncoupled transitions. It is found that in the case of perfect spectral matching of MO to ring resonator, the locking range is independent of the spectral line, whether it be coupled via the cascade or not. These results are derived in Appendix C. There, it is shown that the locking range is given by,

$$\delta_1 = \sqrt{(M^2 - 1)\ P_o/Posc}$$

for all transitions to first order in the perturbations. For a matched system, P_o/P_{osc} is independent of wavelength which implies that δ_1 is the same to first order for all transitions.

The requirement for matching the cavity lengths of the MO and the ring is shown in detail in Appendix C. There it is shown that injection locking on all lines requires,

$$2\pi\ /\lambda\ (l_R - l_L)\ < \delta_1 \quad (\text{MODULO } 2\pi)$$

This will, in general, require that $|l_R - l_L)| < \delta_1/2\pi\bar{\lambda}$, where $\bar{\lambda}$ is the mean wavelength of the spectrum. To see the requirement for equal cavity length, consider the case in which the two lengths are matched to an integral number of wavelengths, n, at the mean wavelength $\bar{\lambda}$, with residual phase error.

In this case,

$$2\pi(l_R - l_L) = 2\pi n\bar{\lambda}$$

The optical phase an an adjacent wavelength $\lambda = \bar{\lambda}-\Delta\lambda$ is then,

$$\phi = 2\tau/\lambda\,(l_R - l_L) = 2\pi n\bar{\lambda} \simeq 2\pi n + 2\pi n\,\Delta\lambda/\lambda$$

In order for this line to be locked, we require,

$$\phi < \delta_1 \text{ or } 2\pi n\Delta\lambda/\lambda < \delta_1$$

For representative values, $\Delta\lambda/\lambda = 0.1$, $\delta_1 = 0.1$, we get

$$|n| < 1/2\pi$$

This inequality can only be satisfied for n=o. That is, for a multiline injection locked configuration, it is necessary to match the MO and ring resonator cavity lengths absolutely to an accuracy better than δ_1.

2.5 Reverse Wave Effects

The stable resonator model was employed to determine the relative strength of the reverse wave in various portions of the system as functions of system parameters for two cases of interest. This analysis is detailed in Appendix D and the important results are shown in Figure 15.

The two cases of interest corresponded to a free-running ring with a retro-reflector

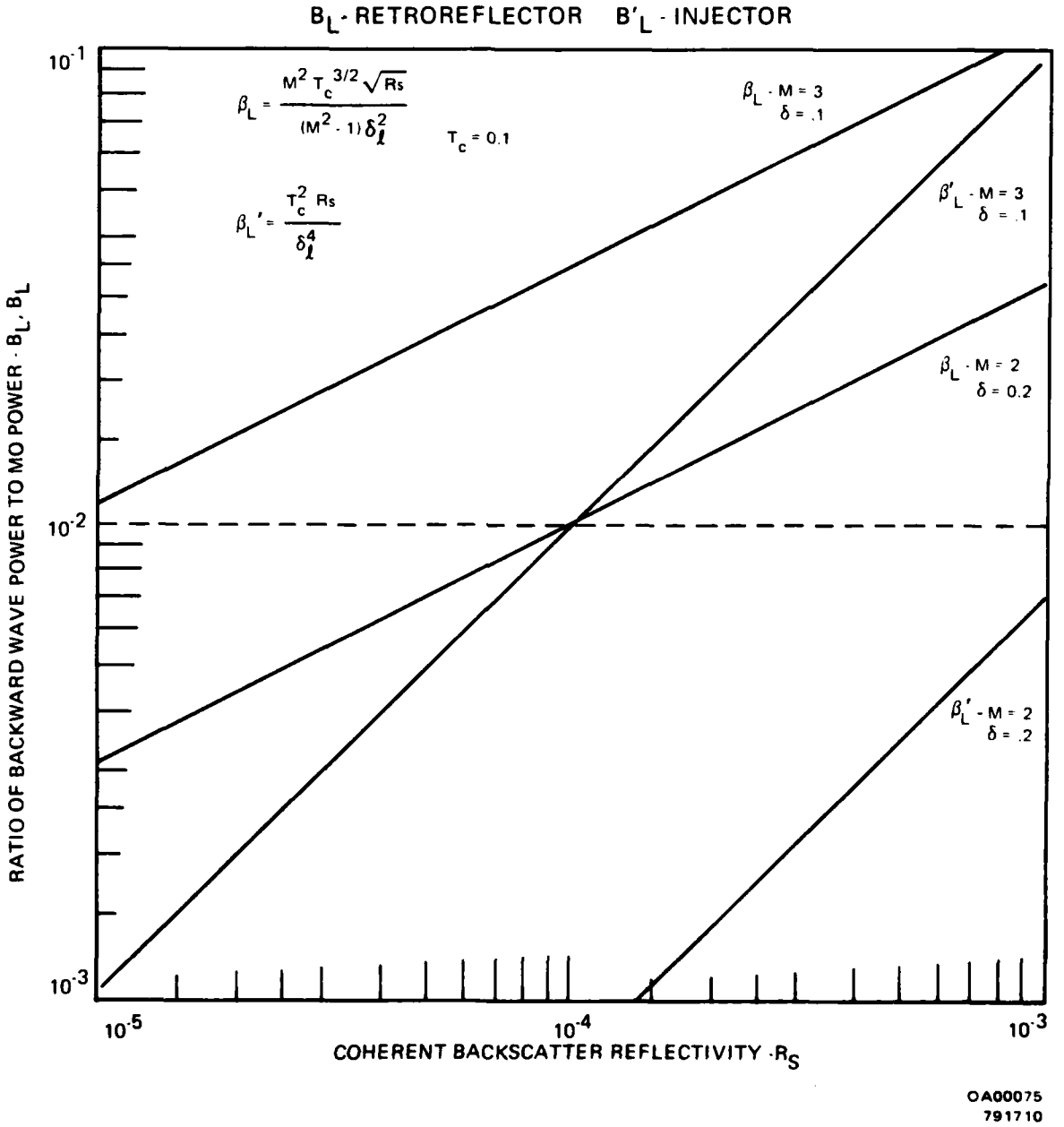

Figure 15. Comparison of Return Wave Suppression

and an injection locked ring with no retro-reflector. The quantities B_L and B'_L for the two cases are the ratios of reverse wave power to MO power at the MO output coupler.

The results shown in Figure 15 indicate that forward wave injection is, in general, a more effective means of suppressing backward wave oscillation than the use of a retro-reflector. The abscissa in this graph, R_s, is the effective reflectivity of any sources of backscatter in the optics, medium or target, if applicable.

The results indicate that it is necessary to limit R_s to 10^{-4} (40 dB) or better in order to guarantee that the power reflected back into the MO is less than .01 of P_o, the MO output.

2.6 Code Development

Beam injection at any optic was added to the bare rectangular SOQ code. This new option allowed the equivalent compacted ring resonator to be analyzed. To analyze the annular ring resonator, the simple w-axicon model and an annular propagation algorithm were necessary. These models were developed, incorporated into the rectangular SOQ, and checked out under another program.

The bare resonator code modifications specific to the injection locking concept were applied to a loaded resonator code (developed under another program). This code contains the necessary HF kinetics and multi-line capability to model a high energy version of the resonator being studied.

3.0 CONCLUSIONS AND RECOMMENDATIONS

3.1 Conclusions

For the equivalent compacted ring resonator, beam injection can help maintain bare resonator power coupling at the unperturbed value. For small misalignments, injection improves bare beam quality, but it does not improve quality degradation due to astigmatism.

For the annular ring resonator, beam injection maintains both bare resonator power coupling and beam quality at the unperturbed values for very small misalignments. And, as expected, this resonator is much more sensitive to misalignment than its equivalent compacted resonator. Additionally, the reverse wave analysis has shown the unstable ring/linear stable MO injection configuration to offer satisfactory reverse wave suppression.

3.2 Recommendations

Based on bare resonator analyses injection locking shows promise. To determine its potential, loaded resonator analyses for high-power devices must be performed. Mode discrimination, possible parasitics, sensitivity to misalignment, and scaleability to high power are potential problems that need in-depth investigation. Additionally, the technical issues associated with cavity length equalization to less than λ; matching of the MO and HEL spectra; and the stability, mode matching and power requirements for the MO need to be addressed experimentally so the real hardware requirements can be established.

APPENDIX A

INJECTION CONTROLLED OPTICAL CONFIGURATION

I. GEOMETRIC OPTICS ANALYSIS

The object of the analysis is to develop equations for selecting parameter values and layout for computer code calculations. Also, to develop a compacted equivalent for the annular ring resonator. Assuming that:

D_b = Outer diameter of annular gain region

D_a = Inner diameter of annular gain region

ℓ = Length of annular gain region

R_2, R_1 = Confocal cavity radii of curvature

D_2 = Injected beam diameter for axial injection

D_c = Inner diameter of hole coupler

D_2/M = Inner diameter of injected beam

$2d = D_b - D_a$

$\ell_1, \ell_2, \ell_3, \ell_4, \ell_5, \ell_6, \ell_7$ = Length of ring resonator portions as shown on Figure 1

The compacted equivalent in the absence of the injection coupling hole is a confocal asymmetric ring: Using the notation of Freiberg,et. al.[1]

$L_2 = \ell_1 + \ell_2$

$L_3 = \ell_3 + \ell_4 + \ell_5 + \ell_6$

$M = R_2/R_1 \quad L_1 = \frac{1}{2}(R_2 - R_1)$

$2a = D_c$

---

1. Freiberg, et. al., IEEE J. Quant. Electr. QE-10,2, (1974).

then,

$$N_{eq} = \frac{D_c^2/4\ (R_2^2 - R_1^2)}{\lambda\ \left[R_1^2 R_2\ (R_2 - R_1) + 2R_2^2 L_2 + 2R_1^2 L_3\right]} \qquad (1)$$

$$= \frac{D_c^2\ (M^2 - 1)}{8\lambda\ \left[ML_1 + M^2 L_2 + L_3\right]}$$

$$MD_c = D_2 + 2_d = D_2 + D_b - D_a$$

As the coupling hole diameter is increased, with fixed gain medium geometry and cavity magnification, the equivalent Fresnel number increases.

$$\text{e.g.} \quad N_{eq} = \frac{(D_2 + 2d)^2\ (M^2 - 1)}{8\lambda\ M^2\ \left[ML_1 + M^2 L_2 + L_3\right]} \qquad (2)$$

II. GEOMETRIC MODE MATCHING

The geometric mode of the ring resonator has a uniform intensity distribution in the collinated portion of the compacted ring. The conjecture is that the injected intensity should match the circulating intensity for a self consistent solution above threshold.

In the diagram below, where P_2, P_1 are the output and input powers for the compacted annular gain medium and P_i is the injected power and all intensity distributions are uniform;

Employing a homogeneous gain saturation model gives,

$$P_2 = GP_1 = G_0 P_1 \, e^{-(P_2 - P_1)/P_{sat}} \tag{3}$$

G, G_0 = saturated and small signal power gains.

P_{sat} = saturation power

Equalizing intensities at the injection port,

$$P_2 = \frac{M^2 D_c^2 - D_2^2}{D_2^2 (1 - 1/M^2)} \, P_i \tag{4}$$

and for purely geometric ouput coupling,

$$P_1 = P_0 + P_2 \frac{D_c^2 - D_2^2}{M^2 D_c^2 - D_2^2} \tag{5}$$

solving for P_1 in terms of P_0 gives,

$$P_1 = \left[1 + \left(\frac{D_c^2 - D_2^2}{M^2 D_c^2 - D_2^2} \right) \left(\frac{M^2 D_c^2 - D_2^2}{D_2^2 - D_2^2/M^2} \right) \right] P_0 \tag{6}$$

and

$$P_2 = \frac{M^2 D_c^2 - D_2^2}{D_2^2 (1 - 1/M^2)} \, P_0 \tag{7}$$

let $D_c / D_2 = m$

then,

$$P_1 = \left[1 + \left(\frac{m^2 - 1}{m^2 M^2 - 1}\right)\left(\frac{m^2 M^2 - 1}{1 - 1/M^2}\right)\right] P_0$$

$$= \left(\frac{m^2 M^2 - 1}{M^2 - 1}\right) P_0 \qquad (8)$$

and,

$$P_2 = M^2 \left(\frac{m^2 M^2 - 1}{M^2 - 1}\right) P_0 = M^2 P_1 \qquad (9)$$

also,

$$\frac{P_2}{P_1} = M^2 = G_0 \, e^{-(P_2 - P_1)/P_{sat}}$$

but

$$P_2 - P_1 = (M^2 - 1)\left(\frac{m^2 M^2 - 1}{M^2 - 1}\right) P_0 = (m^2 M^2 - 1) P_0$$

and,

$$M^2 = G_0 \, e^{-(m^2 M^2 - 1) P_0 / P_{sat}}$$

$$(m^2 M^2 - 1) P_0 = (\ln G_0 - 2 \ln M) P_{sat}$$

$$P_0 = \frac{(\ln G_0 - 2 \ln M)}{(m^2 M^2 - 1)} P_{sat} \qquad (10)$$

$$= \frac{\Delta P}{\left(m^2 M^2 - 1\right)} \qquad (11)$$

where ΔP is the power extracted from the gain medium. Note that this is the same power that would be extracted if there were no injection coupling. The total ouput power is just $P_0 + \Delta P$.

$$P_{out} = P_0 + \Delta P = \left(1 + \frac{1}{m^2 M^2 - 1}\right) \Delta P \simeq \Delta P = P_{osc}.$$

An interesting result is that if $\ln G_0 < 2 \ln M$ and the ring resonator is below threshold, then there is no solution to equation (10) for P_0. Physically this implies that there is no uniform intensity solution for below threshold regenerative amplification in the axial coupled ring unstable resonator.

Equation (11) yields a compact equation for the required injected power in terms of the self-oscillation power of the device $P_{osc} \simeq \Delta P$, the resonator confocal magnification M, and the ratio of the output coupling diameter to injection coupling diameter $m = D_c/D_2$.

$$P_0 = \frac{P_{osc}}{m^2 M^2 - 1} \tag{12}$$

An estimate for the injection locking phase range in radians can be made by analogy with the result for a stable ring with a dielectric coupler of reflectivity R. In the case under study the injected power enters via a second coupler with R=1. The equation is,

$$\delta = \sqrt{\frac{1 - r^2}{r^2} \frac{P_0}{P_{osc}}} \tag{13}$$

where, $r = \sqrt{R}$; pursuing the analogy for an unstable ring $r = \frac{1}{M}$ in the geometric limit

$$\delta = \sqrt{\frac{1 - 1/M^2}{1/M^2} \frac{P_0}{P_{osc}}} = \sqrt{(M^2 - 1) \frac{P_0}{P_{osc}}}$$

When this result is combined with equation (12),then,

$$\delta = \sqrt{\frac{M^2 - 1}{m^2 M^2 - 1}} \tag{14}$$

That is, if the injected power is chosen to match the free running intensity, the injection locking phase range will be a function only of the magnifications M and m.

Note that there are certain interesting values for m given by

$$m = M^n \qquad n = 0,1,2,3...$$

n is the number of round trips required for the injected beam to fill the output coupler inner diameter. For these special cases,

$$\frac{P_0}{P_{osc}} = \frac{1}{M^{2n+2} - 1}$$

$$\delta = \sqrt{\frac{(M^2 - 1)}{M^{2n+2} - 1}}$$

APPENDIX B

IMPORTANT GAIN RELATIONSHIPS FOR THREE LEVEL CASCADE GAIN MEDIUM

In this section the three line gain saturation expressions for a cascading set of levels is derived. Velocity effects and the spatial dependence of the populations are neglected and the solutions are limited to steady state conditions. The results are then applied to multi-line power extraction in regenerative amplifiers.

The rate equations for the populations of the three livels N_1, N_2, N_3 and the ground state N_0 are:

$$(1.a) \qquad \frac{dN_1}{dt} = R_{10} + N_2\omega_{21} + \omega_{21}(N_2 - N_1) - W_{10}(N_1 - N_0) - N_1\omega_{10}$$

$$(1.b) \qquad \frac{dN_2}{dt} = R_{20} + N_3\omega_{32} + W_{32}(N_3 - N_2) - N_2\omega_{21} - W_{21}(N_2 - N_1)$$

$$(1.c) \qquad \frac{dN_3}{dt} = R_3 - N_3\omega_{32} - W_{32}(N_3 - N_2)$$

and $\qquad N = N_0 + N_1 + N_2 + N_3$ = total density of molecules.

Note that additional pumping and relaxation terms can be added to equations (1) without changing the basic results of the analysis.

In the steady state $\frac{dN_1}{dt} = \frac{dN_2}{dt} = \frac{dN_3}{dt} = 0$ and,

$$(2.a) \qquad R_1 + N_2\omega_{21} + W_{21}(N_2 - N_1) - W_{10}(2N_1 + N_2 + N_2 - N) - N_1\omega_{10} = 0$$

$$(2.b) \qquad R_2 + N_3\omega_{32} + W_{32}(N_3 - N_2) - N_2\omega_{21} - W_{21}(N_2 - N_1) = 0$$

$$(2.c) \qquad R_3 - N_3\omega_{32} - W_{32}(N_3 - N_2) = 0$$

Solving for $W_{21}(N_2-N_1)$, $W_{10}(N_1-N_0)$, $W_{32}(N_3-N_2)$ which are proportional to gain per unit length.

$$(\omega_{10}+2W_{10}+W_{21})\,N_1 + (W_{10}-W_{21}-\omega_{21})\,N_2 + (W_{10})\,N_3 = R_1 + W_{10}N$$

$$(-W_{21})\,N_1 + (\omega_{21} + W_{21} + W_{32})\,N_2 + (-\omega_{32} - W_{32})\,N_3 = R_2$$

$$(0)\,N_1 + (-W_{32})\,N_2 + (\omega_{32} + W_{32})\,N_3 = R_3$$

$$\Delta = \begin{vmatrix} \omega_{10} + 2W_{10} + W_{21} & W_{10} - (\omega_{21} + W_{21}) & W_{10} \\ -W_{21} & W_{32} + (\omega_{21} + W_{21}) & -(\omega_{32} + W_{32}) \\ 0 & -W_{32} & (\omega_{32} + W_{32}) \end{vmatrix}$$

$$= (\omega_{32} + W_{32}) \left[\omega_{10} W_{21} + 2\omega_{21} W_{10} + {}_{10} W_{21} + 3W_{10} W_{21}\right] + W_{10}W_{21}W_{32}$$

$$\Delta_1 = \begin{vmatrix} (R_1 + W_{10}N) & W_{10} - (\omega_{21} + W_{21}) & W_{10} \\ R_2 & W_{32} + (\omega_{21} + W_{21}) & -(\omega_{32} + W_{32}) \\ R_3 & -W_{32} & (\omega_{32} + W_{32}) \end{vmatrix}$$

and:

$$\Delta_1 = -(R_2 + R_3)\,W_{10}\,(\omega_{32} + 2W_{32}) + (\omega_{32} + W_{32})(R_1 + R_2 + R_3 + W_{10}N)$$
$$-R_3\,W_{10}\,(\omega_{21} + W_{21})$$

$$= (\omega_{21} + W_{21})(\omega_{32} + W_{32})(R + NW_{10}) - W_{10}\,(\omega_{32} + 2N_{32})(R_2 + R_3)$$
$$- R_3\,W_{10}\,(\omega_{21} + W_{21})$$

where $R = R_1 + R_2 + R_3$

Similarly,

$$\Delta_2 = (\omega_{10} + 2W_{10})(\omega_{32} + W_{32})(R_2 + R_3) - R_3\,W_{10}\,W_{21}$$
$$+ W_{21}\,(R + NW_{10})(\omega_{32} + W_{32})$$

and:

$$\Delta_3 = (\omega_{10} + 2N_{10})(\omega_{21} + W_{21})R_3 + W_{21}\,W_{32}\,(R + NW_{10})$$
$$+ R_3\,W_{10}\,W_{21} + W_{32}\,(\omega_{10} + 2W_{10})(R_2 + R_3)$$

now,

$$\Delta_3-\Delta_2= \left[\omega_{21}R_3 - W_{32}\ (R_2 + R_3)\right]\ \left[\omega_{10} + 2W_{10}\right]\ +\ \left[\omega_{10}\ R_3 - (R_1 + R_2 + {}_3\ R\ )\omega_{32}\right] W_{21}$$

$$+\ \left[4R_3 - \omega_{32}N\right]\ W_{10}\ W_{21}$$

and,

$$\Delta_2-\Delta_1= (\omega_{10} + 2W_{10})(\omega_{32} + W_{32})(R_2 + R_3) - R_3W_{10}W_{21}$$

$$+ W_{21}\ (R+NW_{10})(\omega_{32} + W_{32}) - (\omega_{21} + W_{21})(\omega_{32} + W_{32})(R+NW_{10})$$

$$+ W_{10}\ (\omega_{32} + 2W_{32})(R_2 + R_3) + R_3W_{10}\ (\omega_{21} + W_{21})$$

also,

$$\Delta_1-\Delta_0= \left[2R_1\omega_{21}\omega_{32} + 2\omega_{21}\omega_{32}(R_2 + R_3) + \omega_{10}\omega_{32}\ (R_2 + R_3)\right.$$

$$\left.+\omega_{10}\omega_{21}R_3 - \omega_{10}\omega_{21}\omega_{32}N\right]$$

$$+ \left[3\ (R_1 + R_2 + R_3)\ \omega_{32} + \omega_{10}R_3 - \omega_{10}\omega_{32}N\right]\ W_{21}$$

$$+ \left[2\ (R_1 + R_2 + R_3)\ \omega_{21} + 2\ (R_2 + R_3)\ \omega_{10} - \omega_{10}\omega_{21}\ N\right]\ W_{32}$$

$$+ \left[4\ (R_1 + R_2 + R_3) - \omega_{10}N\right]\ W_{21}W_{32}$$

$$(N_1-N_0)= \frac{\left[\frac{2R}{\omega_{10}} + \frac{R_2+R_3}{\omega_{21}} + \frac{R_3}{\omega_{32}} - N\right] + \left[\frac{3R}{\omega_{10}} + \frac{R_3}{\omega_{32}} - N\right]\frac{W_{21}}{\omega_{21}} + \left[\frac{2R}{\omega_{10}} + \frac{2(R_2+R_3)}{\omega_{21}} - N\right]\frac{W_{32}}{\omega_{32}} + \left[\frac{4R}{\omega_{10}} - N\right]\frac{W_{21}}{\omega_{21}}\frac{W_{32}}{\omega_{32}}}{\left(1 + \frac{W_{32}}{\omega_{32}}\right)\left[1 + 2\frac{W_{10}}{\omega_{10}} + \frac{W_{21}}{\omega_{21}} + 3\frac{W_{10}}{\omega_{10}}\frac{W_{21}}{\omega_{21}}\right] + \frac{W_{10}W_{21}W_{32}}{\omega_{10}\omega_{21}\omega_{32}}}$$

$$\frac{W_{22}}{\omega_{22}} = I_{2/I_{1_{sat}}} \equiv I_2 \qquad \text{(Understood that all intensities are normalized to saturation values)}$$

$$\frac{W_{32}}{\omega_{32}} \equiv I_3 \ ; \ \frac{W_{10}}{\omega_{10}} = I_1$$

then,

$$N_1-N_0 = \frac{\left[\frac{2R}{\omega_{10}} + \frac{R_2+R_3}{\omega_{21}} + \frac{R_3}{\omega_{32}} - N\right] + \left[\frac{3R}{\omega_{10}} + \frac{R_3}{\omega_{32}} - N\right]I_2 + \left[\frac{2R}{\omega_{10}} + \frac{2(R_2+R_3)}{\omega_{21}} - N\right]I_3 + \left[\frac{4R}{\omega_{10}} - N\right]I_2I_3}{\left(1 + I_3\right)\left[1 + 2I_1 + I_2 + 3I_1I_2\right] + I_1I_2I_3}$$

similarly

$$N_2 - N_1 = \frac{\left[\frac{R_2+R_3}{\omega 21} - \frac{R_1+R_2+R_3}{\omega 10}\right](1+I_3)+\frac{1}{2}\left[\frac{R_3}{\omega 32}+3\frac{(R_3+R_2)}{\omega 21}-N\right] I_1+\frac{1}{2}\left[\frac{4(R_2+R_3)}{\omega 21}-N\right] I_1 I_3}{(1+I_3)\left[1+2I_1+I_2+3I_1I_2\right]+I_1I_2I_3}$$

and

$$N_2 - N_3 = \frac{\left[\frac{R_3}{\omega 32}-\frac{(R_2+R_3)}{\omega 21}\right](1+I_1)+\left[\frac{R_3}{\omega 32}-\frac{R}{\omega 10}\right] I_2+\frac{1}{2}\left[\frac{R}{\omega 32}-N\right] I_1 I_2}{(1+I_1)(1+I_2)(1+I_3)+\frac{1}{2}(1+2I_3) I_1 I_2}$$

Making the following identifications

(1) Uncoupled small signal gain per unit length of transition 1→0 alone.

($I_2 = I_3 = 0$)

$$g_o^1 = \left[\frac{2(R_1+R_2+R_3)}{\omega 10}+\frac{R_2+R_3}{\omega 21}+\frac{R_3}{\omega 32}-N\right]$$

(2) $$g_o^2 = \frac{R_2+R_3}{\omega 21}-\frac{R_1+R_2+R_3}{\omega 10}$$

(3) $$g_o^3 = \frac{R_3}{\omega_{32}}-\frac{R_2+R_3}{\omega_{21}}$$

Then

$$g^1(I_1,I_2,I_3) = \frac{g_o^1+\left[g_o^1-g_o^2\right]I_2+\left[g_o^1-g_o^3\right]I_3+\left[g_o^1-2g_o^2-g_o^3\right]I_2I_3}{(1+I_1)(1+I_2)(1+I_3)+\frac{1}{2}(1+2I_3)I_1I_2}$$

as the coupled saturated gain on transition 1→0

and

$$g_o^2(I_1,I_2,I_3) = \frac{g_o^2(1+I_3)+\left[g_o^2+\frac{1}{2}g_o^1\right]I_1+\left[g_o^2-\frac{g_o^1-g_o^3}{2}\right]I_1I_3}{(1+I_1)(1+I_2)(1+I_3)+\frac{1}{2}(1+2I_3)I_1I_2}$$

also

$$g^3(I_1,I_2,I_3) = \frac{g_o^3(1+I_1)+\left[g_o^3+g_o^2\right]I_2+\frac{1}{2}\left[3g_o^3+2g_o^2+g_o^1\right]I_1I_2}{(1+I_1)(1+I_2)(1+I_3)+\frac{1}{2}(1+2I_3)I_1I_2}$$

The above expressions must be integrated over the length of the amplifying medium in order to obtain the power gain used in the injection locking equations.

Special Cases

(a)
$$g^1(I_1,o,o) = \frac{g_o^1}{1+I_1}$$
$$g^2(o,I_2,o) = \frac{g_o^2}{1+I_2}$$
$$g^3(o,o,I_3) = \frac{g_o^3}{1+I_3}$$
} Single line gain expressions

(b)
$$g^1(I_1,I_2,o) = \frac{g_o^1 + \left[g_o^1-g_o^2\right] I_2}{(1+I_1)(1+I_2)+\frac{1}{2}I_1I_2}$$
$$g^1(I_1,o,I_3) = \frac{g_o^1 + \left[g_o^1-g_o^3\right] I_3}{(1+I_1)(1+I_3)} = \frac{g_o^1}{1+I_1} - \frac{g_o^3 I_3}{(1+I_1)(1+I_3)}$$
$$g^1(o,I_2,I_3) = \frac{g_o^1 + \left[g_o^1-2g_o^2-g_o^3\right] I_2I_3}{(1+I_2)(1+I_3)+\frac{1}{2}(1+2I_3)I_1I_2}$$
} two line gain expressions

A special case involving a pair of lines that is integrable in closed form series to develop the general results.

Suspose $I_1=0$, $I_2, I_3 \neq 0$

then,
$$g^2 = \frac{g_o^2}{1+I_2}$$
$$g^3 = \frac{g_o^3 + \left[g_o^3+g_o^2\right]I_2}{(1+I_2)(1+I_3)}$$
$$= \frac{g_o^3}{1+I_3} + \frac{g_o^2 I_2}{(1+I_2)(1+I_3)}$$

I. INTEGRATED POWER GAIN EXPRESSIONS FOR CASCADING GAIN MEDIA

Consider the case of two cascading transitions A and B for which the gain per unit length expressions are,

$$g_A = \frac{g_o^A}{1 + P_A} = \frac{1}{P_A}\frac{dP_A}{dZ} \tag{1}$$

$$g_B = \frac{g_o^B}{1 + P_B} + \frac{g_o^A P_A}{(1+P_A)(1+P_B)} = \frac{1}{P_B}\frac{dP_B}{dZ} \tag{2}$$

Power extraction and power gain can be analyzed by examining a single pass through the gain medium.

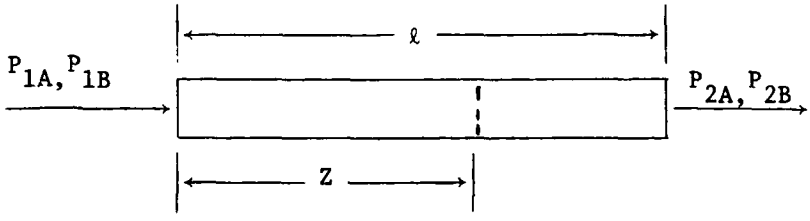

$$(1 + P_A)\frac{dP_A}{P_A} = g_o^A\, dZ$$

$$(1 + P_A)\frac{dP_B}{P_B} = g_o^B\, dZ + dP_A$$

Integration from o→ℓ yields,

$$\ln\left(\frac{P_{2B}}{P_{1B}}\right) + P_{2B} - P_{1B} + P_{1A} - P_{2A} = g_o^B \ell$$

$$\ln\left(\frac{P_{2A}}{P_{1A}}\right) + P_{2A} - P_A = g_o^A \ell$$

but

$$G_A = \frac{P_{2A}}{P_{1A}} = \text{power gain for line A}$$

$$G_B = \frac{P_{2B}}{P_{1B}} = \text{power gain for line B}$$

so,

$$\ln G_B + P_{1B}(G_B-1) - P_{1A}(G_A-1) = \ln G_B^o = g_o^B \ell$$

$$\ln G_A + P_{1A}(G_A-1) - \ln G_A^o = g_o^A \ell$$

Power extracted on line A, $\Delta P_A = (G_A-1)P_{1A}$

$$\Delta P_B = (G_B-1)P_{1B}$$

so,

$$\ln G_B + \Delta P_B - \Delta P_A = g_o^B \ell = \ln G_o^B$$

$$\ln G_A + \Delta P_A = \ln G_o^A = g_o^A \ell$$

and

$$G_B = G_B^o e^{-(\Delta P_B - \Delta P_A)} \tag{3}$$

$$G_A = G_A^o e^{-\Delta P_A} \tag{4}$$

Equation (3) shows that the operating gain on line B is directly related (coupled) to that on line B.

i.e. $$G_B = G_B^o e^{-\Delta P_B} e^{\Delta P_A} = \frac{G_A^o G_B^o}{G_A} e^{-\Delta P_B}$$

These relationships will be used in the analysis of regenerative amplification, injection locking, and return wave suppression.

$$\Delta P_A = g_o^A \ell - \ln G_A$$

$$\Delta P_B = g_o^B \ell + \ln G_B + \Delta P_A$$

If, as in most applications of interest G_A and G_B are approximately equal and determined by the loss per pass then the cascade has resulted in an additional extracted power of ΔP_A in line B.

II. EXPRESSIONS FOR POWER GAIN WITH TWO-WAY PROPAGATION

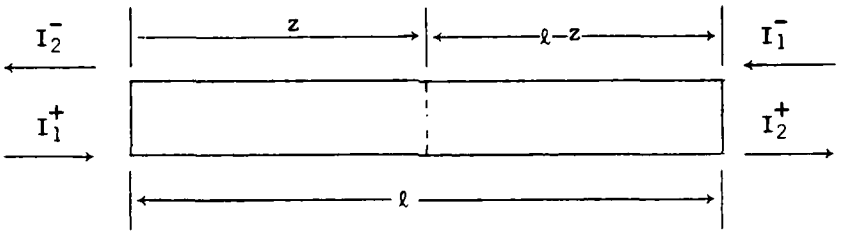

At any point in the medium the net field is

$$I(z) = I^-(z) + I^+(z)$$

The homogeneously saturating gain /cm is,

$$g(z) = \frac{g_o}{1+(I^-+I^+)/I_s}$$

for simplicity normalize all intensities to I_s

$$g(z) = \frac{g_o}{1+I^++I^-}$$

$$\frac{1}{I^+}\frac{dI^+}{dz} = \frac{g_o}{1+I^++I^-} = -\frac{1}{I^-}\frac{dI^-}{dz}$$

where

$$I^+(o) = I_1^+ \; ; \; I^+(\ell) = I_2$$

$$I^-(o) = I_2^- \; ; \; I^-(\ell) = I_1$$

and

$$\frac{I_2^+}{I_1^+} = G^+ \; ; \; \frac{I_2^-}{I_1^-} = G^-$$

in general

$$\frac{1}{I^+}\frac{dI^+}{dz} + \frac{1}{I^-}\frac{dI^-}{dz} = o$$

so that,

$$I^+I^- = I_1{}^+I_2{}^- = I_1{}^-I_2{}^+ = c \text{ (constant)}$$

and

$$G^+ = G^- = G \quad \text{(power gain is symetric)}$$

$$\frac{1}{I^+}\frac{dI^+}{dz}(1+I^++I^-) = g_o$$

$$\frac{dI^+}{I^+} + dI^+ + \frac{I^-}{I^+}dI^+ = g_o dz$$

but

$$I^- = \frac{c}{I^+}$$

so that,

$$\frac{dI^+}{I^+} + dI^+ + c\frac{dI^+}{I^{+2}} = g_o dz$$

After integration from $o \rightarrow \ell$

$$\ln\left(\frac{I_2{}^+}{I_1{}^+}\right) + (I_2{}^+ - I_1{}^+) - c\left(\frac{1}{I_2{}^+} - \frac{1}{I_1{}^+}\right) = g_o\ell$$

Similar result for I^- gives pair of equations,

$$\ln G + I_2{}^- - I_1{}^- - c\left(\frac{1}{I_2{}^-} - \frac{1}{I_2{}^-}\right) = g_o\ell$$

$$\ln G + I_2{}^+ - I_1{}^+ - c\left(\frac{1}{I_2{}^+} - \frac{1}{I_2{}^-}\right) = g_o\ell$$

These equations can be replaced by a single equation,

$$\ln G + (G-1)(I_1^+ + I_1^-) = g_o \ell$$

or

$$G = G_o e^{-(\Delta P^+ + \Delta P^-)}$$

APPENDIX C

MULTILINE INJECTION LOCKING ANALYSIS

The figure below shows the layout for the stable ring resonator/injection locking analysis.

Note that lower case g refers to amplitude gain integrated over the gain medium length; this should not be confused with gain per unit length of previous analyses.

Specifically	Present Symbol	Previous Symbol
power gain	g^2, g_o^2	G, G_o
amplitude gain	g, g_o	G, G_o
gain/length	α, α_o	g, g_o

Referring to the figure, mirrors M_1 and M_2 define the master oscillator cavity which is driven by a gain medium with amplitude gain g_L, L refers to linear cavity. The ring resonator is defined by M_3, M_5, M_6, M_7, M_8 and amplitude gain g_R. M_9 is a retro mirror for enhancement of the forward wave; M_4 is a retro mirror with effective reflectivity r_s to represent a small amount of backscatter in the system that acts as the source of the return wave.

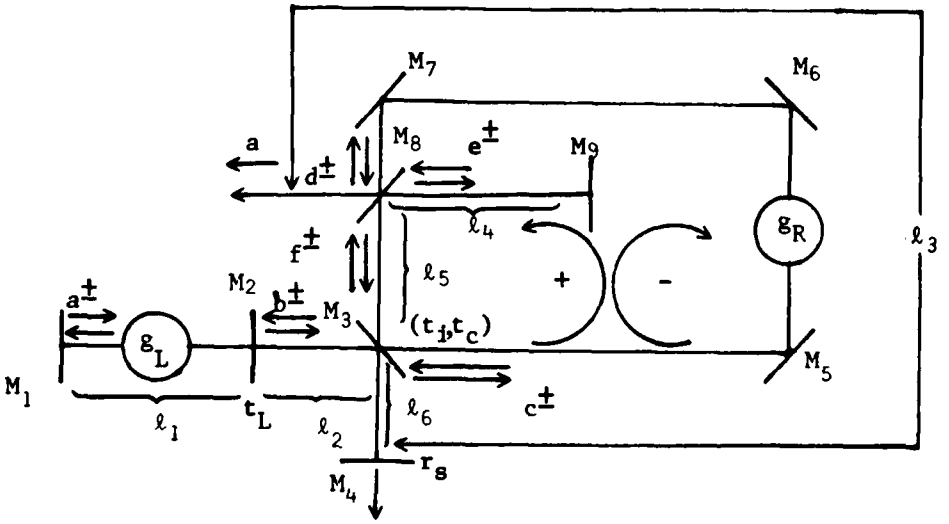

Definition of terms

$\tilde{a}^+, \tilde{b}^+, \tilde{c}^+, \tilde{d}^+, \tilde{f}^+, \tilde{e}^+$ - forward wave amplitudes

$\tilde{a}^-, \tilde{b}^-, \tilde{c}^-, \tilde{d}^-, \tilde{f}^-, \tilde{e}^-$ - backward wave amplitudes

$\tilde{\theta}$ - output wave amplitude

g_L, g_R - operating amplitude gains

t_L = Master oscillator output transmittance (M_2)

r_L = Master oscillator output reflectance (M_2)

t_R = Ring resonator output transmittance (M_8)

r_R = Ring resonator output reflectance (M_8)

k = Wave vector = $\frac{2\pi}{\lambda}$

r_s = Backscatter reflectance (M_4)

Nonreciprocal coupling of injection hole

t_i = *Transmittance of M_3 for injected beam*

t_c = Transmittance of M_3 for backward wave

We have the following set of simultaneous equations for the fields

$$\tilde{a}^+ \left[1 - g_L^2 r_L e^{i2k\ell_1}\right] = -g_L t_L \tilde{b}^- e^{ik\ell_1} \tag{1}$$

$$\tilde{b}^+ = t_L g_L e^{ik\ell_1} \tilde{a}^+ - r_L \tilde{b}^- \tag{2}$$

$$\tilde{c}^- r_c t_R g_R e^{ik(\ell_3+\ell s)} = \tilde{c}^- + \underbrace{t_c t_i t_R g_R r_s e^{ik(2\ell_6+\ell_3+\ell_5)}}_{\text{backscatter}} \tilde{c}^+ \tag{3}$$

$$\tilde{b}^- = t_c e^{ik\ell_2} \tilde{c}^- \tag{4}$$

$$r_c g_R t_R e^{ik(\ell_3+\ell_5)} \tilde{c}^+ - \underbrace{r_R^2 r_c^2 e^{2ik(\ell_5+\ell_4)}}_{\text{retro mirror}} \tilde{c}^- + t_i \tilde{b}^+ e^{ik\ell_2} = \tilde{c}^+ \tag{5}$$

These equations apply to each of the lines of the multiline output.

FORWARD WAVE SOLUTIONS

If r_s=o and there is no backscatter, then equation (3) gives

$$\tilde{c}^- \left[1-r_c t_R g_R e^{ik(\ell_3+\ell_5)}\right] = o$$

The only solution consistent with the other equations is

$$\tilde{c}^- = \tilde{b}^- = o.$$

This is obvious if the retro-mirror is deleted from the system. It can also be shown in the more general case.

The equations for $\tilde{c}^- = \tilde{b}^- = o$ are,

$$g_L^2 r_L e^{i2k\ell_1} = 1$$

$$t_L g_L e^{ik\ell_1} \tilde{a}^+ = b^+$$

$$\tilde{c}^+ = \frac{t_i e^{ik\ell_2}\, \tilde{b}^+}{1-r_c g_R t_R e^{ik(\ell_3+\ell_5)}}$$

This represents operation of the system with complete suppression of the return wave.

Let P_o = MO output power = $\left|\tilde{b}^+\right|^2$

P_{out} = Ring output power = $r_R^2 g_R^2 \left|\tilde{c}^+\right|^2$

but, $$\left|\tilde{c}^+\right|^2 = \left|\frac{t_i^2 P_o}{1-r_c g_R t_R e^{ik(\ell_3+\ell_5)}}\right|^2$$

and,

$$P_{out} = \left|\frac{M_R^2 g_R^2 t_i^2 P_o}{1-r_c g_R t_R e^{ik(\ell_3+\ell_5)}}\right|^2$$

$$= \frac{r_R^2 g_R^2 t_i^2 P_o}{(1+r_c^2 g_R^2 t_R^2) - 2r_c g_R t_R \cos k(\ell_3+\ell_5)}$$

$$= \frac{r_R^2 g_R^2 t_i^2 P_o}{(1-r_c t_R g_R)^2 + 4r_c t_R g_R \sin^2 \frac{k(\ell_3+\ell_5)}{2}}$$

for simplicity let $\ell_3+\ell_5 = \ell_R$ = round trip length of ring

$2\ell_1 = \ell_L$ = round trip length of MO.

The phase shift between the output field $\tilde{\theta}$ and the input $\tilde{b}^+$ is,

$$\Phi = k(\ell_2+\ell_3) + \tan^{-1}\left[\frac{r_c g_R t_R \sin k\ell_R}{1-r_c t_R g_R \cos K\ell_R}\right]$$

so that for the power output and phase of the driven ring output,

$$P_{out} = \frac{M_R^2 g_R^2 t_i^2}{(1-r_c t_R g_R)^2 + 4r_c t_R g_R \sin^2 \frac{k\ell_R}{2}} P_o \qquad (6)$$

$$\Phi = k(\ell_2+\ell_3) + \tan^{-1}\left[\frac{r_c g_R t_R \sin k\ell_R}{1-r_c t_R g_R \cos k\ell_R}\right] \qquad (7)$$

and for unperturbed operation of the MO

$$\dot{g}_L^2 = \frac{e^{-ik\ell_L}}{r_L}$$

In the absence of anomalous dispersion g_L^2 is real and

$$k\ell_L = 2\pi\eta \qquad ,\eta = \text{integer}.$$

This defines the longitudinal mode wavevectors of the MO. A more complete treatment generalizes this result to include the transverse mode structure also. For this analysis the effects of transverse mode wavevector shifts will be neglected. The conclusion, that the longitudinal modes of the ring resonator must be matched to those of the MO, also applies to the transverse modes. Substituting the condition $k\ell_L = 2\pi n$ into (6) and (7),

$$P_{out} = \frac{r_R^2 g_R^2 t_i^2}{(1-r_c t_R g_R)^2 + 4 r_c t_R g_R \, \mathrm{Sin}^2(\pi n \frac{\ell_R}{\ell_L})} \, Po \tag{8}$$

$$\Phi = 2\pi n \frac{(\ell_2+\ell_3)}{\ell_L} + \tan^{-1}\left[\frac{r_c g_R t_R \, \mathrm{Sin}(2\pi n \frac{\ell_R}{\ell_L})}{1-r_c t_R g_R \cos(2\pi n \frac{\ell_R}{\ell_L})}\right] \tag{9}$$

P_{out} will have a global maximum for all wavelengths (i.e. all values of n) if $\ell_R = \ell_L$

$$P_{out}\Big|_{max} = \frac{r_R^2 g_R^2 t_i^2}{(1-r_c t_R g_R)^2} \, P_o \tag{10}$$

From this point on g_R refers to the operating gain at the global maximum for the particular line in question.

The output power of the regenerative amplifier in the injection locked regime differs slightly from that of the free-running oscillator P_{osc}. This motivates the following perturbation analysis; first the single-line uncoupled transition is treated. The results are then extended to the two-line cascade coupled case.

III FORWARD WAVE PERTURBATION ANALYSIS

III.1 Single Wave Analysis

The single line perturbation analysis is simplified by writing the operating gain in terms of the self-oscillating power, P_{osc}. of the ring.

$$g_R = \frac{e^{(P_{osc} - \Delta P)/2}}{r_c t_R} \quad , \quad Posc = \Delta P \text{ gives } r_c t_R g_R = 1 \tag{10}$$

let $$\ell_R = \ell_I + \Delta\ell \quad \frac{2A\eta\Delta\ell}{\ell_I} = k\Delta\ell = \delta$$

then

$$P_{out} = P_o + \Delta P = \left[\frac{r_R^2 g_R^2 t_i^2}{(1 - r_c t_R g_R)^2 + 4 r_c t_R g_R \sin^2 \frac{\delta}{2}} \right] P_o \tag{11}$$

let $$r_c t_R g_R = 1 - \Delta = e^{(Posc - \Delta P)/2}$$

$$\simeq 1 + \frac{1}{2} (P_{osc} - \Delta P)$$

to first order in the perturbations

$$P_o + \Delta P = \frac{r_R^2 g_R^2 t_i^2 P_o}{\Delta^2 + 4 \sin^2 \frac{\delta}{2}} (1 - \Delta)$$

but $2\Delta + \Delta P - Posc$ = increase in extracted power above self oscillation.

$$P_o + Posc + 2\Delta = \frac{r_R^2 g_R^2 t_i^2 P_o}{\Delta^2 + 4(1-\Delta)\sin^2 \frac{\delta}{2}}$$

Consider the region in which the ring can be considered injection locked to the MO. Here $\delta << 1$ and $2\Delta + P_o << P_{osc}$.

$$\Delta^2 + \delta^2 = r_R g_R t_i \frac{P_o}{P_{osc}}$$

$$\Delta^2 \simeq \left(\frac{r_R^2 t_i^2}{r_c^2 t_R^2} \frac{P_o}{P_{osc}} - \delta^2 \right)$$

$$\Delta \simeq \sqrt{\frac{r_R^2 t_i^2}{r_c^2 t_R^2} \frac{P_o}{P_{osc}} - \delta^2}$$

and we can write,

$$P_{out} \simeq P_o + \Delta P$$

$$= P_o + P_{osc} + 2\sqrt{\frac{r_R^2 t_i^2}{r_c^2 t_R^2} \frac{P_o}{P_{osc}} - \delta^2}$$

defining locking phase angle

$$\delta_\ell = \frac{r_R t_i}{r_c t_R} \sqrt{\frac{P_o}{P_{osc}}}$$

then,

$$P_{out} \simeq P_o + P_{osc} + 2\sqrt{\delta_\ell - \delta^2}$$

which is valid for $|\delta| < \delta_\ell$.

When $|\delta| \geq \delta_\ell$ self oscillation of the ring resonator ensues and the driven power decreases. In this regime

$$r_c t_R g_R = 1$$

Driven output

$$P_{out} = \frac{r_R^2 g_R^2 t_i^2}{4 \sin^2 \delta/2} P_o$$

$$= \frac{r_R^2 t_i^2}{r_c^2 t_R^2} \frac{P_o}{4 \sin^2 \frac{\delta}{2}}$$

$$= \frac{\delta_\ell^2 / 4}{\sin^2 \delta/2} \quad P_{osc}$$

note that at

$$\delta = \delta_\ell \ , \quad P_{out} \simeq P_{osc}$$

Driven power decreases rapidly for $\delta > \delta_\ell$. In the limit as $\delta \to \pi$

$$P_{\substack{out \\ \delta \to \pi}} = \delta_\ell^2/4 \ P_{osc} = \frac{r_R^2 t_i^2}{r_c^2 t_R^2} P_o \sim P_o$$

and the coherent power gain is essentially unity.

The phase angle can be treated by the same perturbation approach. Neglecting the linear phase term $2\pi\eta \frac{\ell_2+\ell_3}{\ell_L}$,

$$\Phi(\delta) \simeq \tan^{-1} \left[\frac{r_c g_R t_R \sin \delta}{1 - r_c g_R t_R \cos \delta} \right]$$

In the locking region,

$$\cos \delta \simeq 1 - \frac{\delta^2}{2} \qquad \sin \delta \simeq \delta$$

$$r_c g_R t_R \simeq 1 - \Delta = 1 - \sqrt{\delta_\ell^2 - \delta^2}$$

and

$$\Phi(\delta) \simeq \tan^{-1} \left[\frac{\delta}{\sqrt{\delta_\ell^2 - \delta^2}} \right]$$

In this approximation $\Phi(\delta) \simeq \frac{\delta}{\delta_\ell}$ for $\delta << \delta_\ell$

and $\Phi(\delta) \simeq \pi/2$ when $\delta = \delta_\ell$

Outside the locking region

$$\Phi(\delta) = \tan^{-1} \left[\frac{\sin \delta}{1 - \cos \delta} \right]$$

$$= \cot \frac{\delta}{2}$$

so that

$$\Phi(\delta) = \frac{\pi}{2} + \frac{\delta}{2} \qquad \text{for} \qquad \delta > \delta_\ell .$$

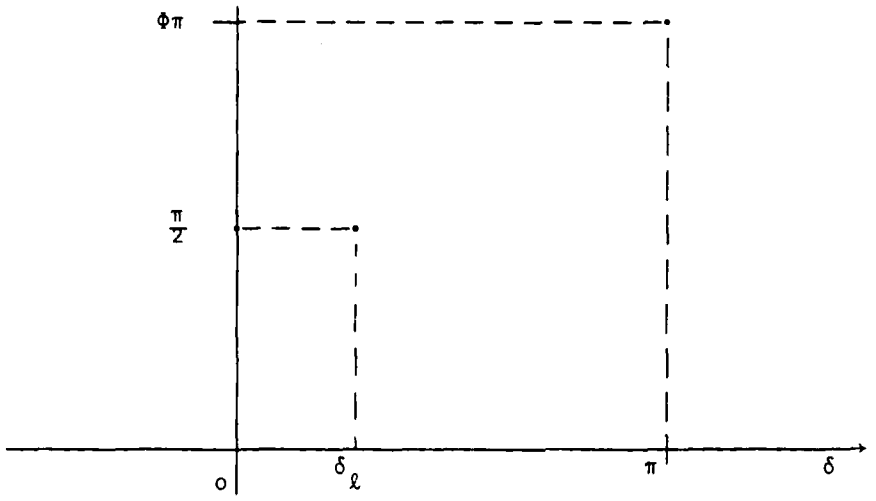

III.2 CASCADE COUPLED LINES ANALYSIS

Consider a pair of cascade coupled lines, A and B. According to the results above,

(a) $$g_{RA} = g^{o}_{RA}\, e^{-\Delta PA/2}$$

(b) $$g_{RB} = g^{o}_{RB} e^{-(\Delta P_B - \Delta P_A)/2}$$

Assume MO output powers P_{oA} and P_{oB} and that r_R, r_c, t_R, t_i, apply to both A and B.

The analysis for line A is indentical to the prededing analysis for the single line case, since it is uncoupled from line B. For line B, then,

$$r_c t_R\, g_{RB} = e^{[(P^{B}_{osc} - \Delta P_B) - (P^{A}_{osc} - \Delta P_A)]/2}$$

$$= 1 - \Delta_B \approx 1 + \tfrac{1}{2}\,(P^{B}_{osc} - \Delta P_B) - \tfrac{1}{2}\,(P^{A}_{osc} - \Delta P_A)$$

or $$2\Delta_B = (\Delta P_B - P^{B}_{osc}) - 2\Delta_A$$

In the injection locked regime,

$$\Delta P_{oB} + \Delta P_B = \frac{r_R^2 g_{RB}^2 \; t_i^2 P_{oB}}{\Delta_B^2 + \Delta_B^2} \qquad \delta_B = k_B \Delta \ell$$

but

$$\Delta P_B = P_{osc}^{B} + 2\Delta_B + 2\Delta_A$$

and

$$P_{oB} + P_{osc}^{B} + 2\Delta_B + 2\Delta_A = \frac{r_R^2 g_{RB}^2 t_i^2 P_{oB}}{\Delta_B^2 + \delta_B^2}$$

In the spirit of the single line analysis $P_{osc} >> P_{oB} + 2\Delta_B + 2\Delta_A$

and

$$P_{osc}^{B} = \frac{r_R^2 g_{RB}^2 t_i^2 P_{oB}}{\Delta_B^2 + \delta_B^2}$$

$$\Delta_B \simeq \sqrt{\frac{r_R^2 t_i^2}{r_c^2 t_R^2} \; \frac{P_{oB}}{P_{osc}^{B}} - \delta_B^2}$$

$$P_{out}^{B} = P_{oB} + \Delta P_B$$

$$= P_{oB} + P_{osc}^{B} + 2 \sqrt{\frac{r_R^2 t_i^2}{r_c^2 t_R^2} \; \frac{P_{oB}}{P_{osc}^{B}} - \delta_B^2} + 2 \sqrt{\frac{r_R^2 t_i^2}{r_c^2 t_R^2} \; \frac{P_{oA}}{P_{osc}^{A}} - \delta_A^2}$$

Define

$$\delta_{\ell A}^2 = \frac{r_R^2 t_i^2}{r_c^2 t_R^2} \; \frac{P_{oA}}{P_{osc}^{A}} \qquad \delta_{\ell B}^2 = \frac{r_R^2 t_i^2}{r_c^2 t_R^2} \; \frac{P_{oB}}{P_{osc}^{B}}$$

then,

$$P_{out}^{B} \simeq P_{oB} + P_{osc}^{B} + 2 \sqrt{\delta_{\ell B}^2 - \delta_B} + 2 \sqrt{\delta_{\ell A}^2 - \delta_A}$$

which is valid for $|\delta| < \delta_\ell$ for both lines.

If the MO spectrum is matched to that of the ring resonator

$$\frac{P_{oA}}{P_{osc}^{A}} = \frac{P_{oB}}{P_{osc}^{B}} \qquad \text{and} \qquad \delta_{\ell A} = \delta_{\ell B}$$

furthermore

$$\delta_{A/\delta_B} = k_{A/k_B} \simeq 1$$

so,

$$P_{out}^{B} \simeq P_{oB} + P_{osc}^{B} + 4\sqrt{\delta_{\ell}^2 - \delta^2}$$

$$P_{out}^{A} \simeq P_{oA} + P_{osc}^{A} + 2\sqrt{\delta_{\ell}^2 - \delta^2}$$

As a result of the cascade coupling, line B has double the sensitivity to change in δ that line A has in the output power.

Outside the locking range $r_c t_R g_{RB} = 1$ and

$$P_{out}^{B} \simeq \frac{r_R^2 t_i^2}{r_c^2 t_R^2} \frac{P_{oB}}{4 \sin^2 \frac{\delta_B}{2}} = \frac{\delta^2 \ell/4}{\sin^2 \delta/2} P_{osc}^{B}$$

which is the same result obtained in the single line analysis. This holds true for the behavior of the phase angle outside the locking range; i.e. it is identical to that for the single line case.

Within the locking range, the phase angle for line B can be obtained by perturbation of

$$\phi(\delta_B) = \text{Tan}^{-1}\left[\frac{r_c g_{RB} t_R \sin \delta_B}{1 - r_c g_{RB} t_R \cos \delta_B}\right]$$

$$r_c g_{RB} t_R \simeq 1 - \Delta_B = 1 \sqrt{\delta_{\ell B}^2 - \delta_B^2}$$

and

$$\phi(\delta_B) \simeq \text{Tan}^{-1}\left[\frac{\delta_B}{\sqrt{\delta_{\ell B}^2 - \delta_B^2}}\right]$$

which is the identical result as in the single line case.

The results of this analysis can be summarized by stating that the effect of coupling between transitions alters the power vs tuning curve from that of the isolated lines. To first order in the injected signal however, there is no change in the phase angle vs tuning curve.

APPENDIX D

RETURN WAVE EFFECTS IN INJECTION LOCKING

Field equations for the injection controlled ring are:

$$\tilde{a}^{+}\left[1 - g_L^2 r_L e^{ik\ell_L}\right] = -g_L t_L \tilde{b}^{-} e^{ik\ell_L/2} \tag{1}$$

$$\tilde{b}^{+} = t_L g_L e^{ik\ell_L/2}\ a^{+} - r_L \tilde{b}^{-} \tag{2}$$

$$\tilde{c}^{-} r_c t_R g_R e^{ik\ell_R} = \tilde{c}^{-} + \underbrace{t_c t_i t_R g_R M_s}_{\text{backscatter}} \underbrace{e^{ik(\ell_R+2\ell_6)}}\ \tilde{c}^{+} \tag{3}$$

$$\tilde{b}^{-} = t_c e^{ik\ell_2}\ \tilde{c}^{-} \tag{4}$$

$$r_c g_R t_R e^{ik\ell_R}\ \tilde{c}^{+} - \underbrace{r_R^2 r_c^2 e^{i\,2k\,(\ell_5 + \ell_4)}}_{\text{retro mirror}}\ \tilde{c}^{-} \tag{5}$$

$$+ t_i \tilde{b}^{+} e^{ik\ell_2} = \tilde{c}^{+}$$

for simplicity assume all MO power is injected into ring t_i=1, also assume that backward wave coupling is weak.

i.e. $\quad r_c = 1 \quad t_c \ll 1.$

then (3) and (5) become

$$\tilde{c}^{-}\left[t_R g_R e^{ik\ell_R} - 1\right] = t_c t_R g_R r_s\ e^{ik\,(\ell_R + 2\ell_6)}\ \tilde{c}^{+} \tag{6}$$

$$\tilde{c}^{+}\left[g_R t_R e^{ik\ell_R} - 1\right] + \tilde{b}^{+} e^{ik\ell_2} = r_R^2 e^{ik(\ell_R+2\ell_6)}\ \tilde{c}^{-} \tag{7}$$

If $\tilde{c}^-$ is regarded as a perturbation resulting from r_s and $\tilde{c}^-$ is computed for two cases:

I. Undriven Ring with Retro-Mirror

In this case $\tilde{b}^+ = 0$ and

$$\tilde{c}^- \left[g_R t_R e^{ik\ell_R} - 1 \right] = t_c t_R g_R r_S \, e^{ik(\ell_R + 2\ell_6)} \tilde{c}^+$$

$$\tilde{c}^+ \left[g_R t_R e^{ik\ell_R} - 1 \right] = r_R^2 e^{i2k(\ell_5 + \ell_4)} \tilde{c}^-$$

then $$\frac{\tilde{c}^-}{\tilde{c}^+} = \frac{t_c t_R g_R r_s}{r_R^2} \frac{\tilde{c}^+}{\tilde{c}^-}$$

In terms of absolute magnitude

$$\frac{\left|\tilde{c}^-\right|^2}{\left|\tilde{c}^+\right|^2} = \frac{t_c t_R g_R r_s}{r_R^2} \tag{8}$$

In the weak return wave limit $g_R t_R \simeq 1$ and

$$\beta_R = \frac{\left|\tilde{c}^-\right|^2}{\left|\tilde{c}^+\right|^2} = \frac{t_c r_s}{r_R^2} = \frac{\sqrt{T_c R_s}}{R_R} \tag{9}$$

= ratio of return to forward wave power

Then the suppression of the return wave in the undriver ring resonator is independent of the phasing of the retro-mirror!

The power incident on the MO due to this backward wave is just,

$$\left|b^-\right|^2 = t_c \left|\tilde{c}^-\right|^2 = \beta_R t_c^2 \left|\tilde{c}^+\right|^2$$

$$= \beta_R t_c^2 \frac{Posc}{r_R^2 g_R^2} \simeq \frac{\beta F T_c T_r Posc}{R_R} \tag{10}$$

The ratio of return to forward power for the MO in this case can be written as,

$$\beta_R = \frac{\left|\tilde{b}^- 1\right|^2}{\left|\tilde{b}^+\right|^2} = \frac{\beta F}{R_R} T_c T_R \quad \frac{Posc}{Po}$$

$$= \frac{\sqrt{T_c R_s}}{R_R^2} \quad T_c T_R \left(\frac{Posc}{P_o}\right) \tag{11}$$

Neglecting any suppression of the return wave due to the injected signal. This isolates the effectiveness of the retro-mirror in the suppression of the backward wave. Equation (11) can be rewritten in terms of the forward wave injection locking angle δ_i,

$$\beta_L = \frac{\sqrt{T_c R_s}}{R_R} \quad T_c \quad \frac{1}{\delta_\ell^2} \tag{12}$$

Next, consider the other regime in which the retro-reflective is not employed, and only the injected beam is relied upon to suppress the backward wave.

In this case equations (6) and (7) become,

$$\tilde{c}^- \left[t_R g_R e^{-ik\ell_R} 1\right] = t_c t_R g_R r_s e^{ik(\ell_R + 2\ell_6)} \tilde{c}^+ \tag{13}$$

$$\tilde{c}^+ \left[t_R g_R e^{ik\ell_R} 1\right] + \tilde{b}^+ e^{ik\ell_2} = 0 \tag{14}$$

Solving for $\left|\tilde{c}^-\right|^2$ gives.

$$\left|\tilde{c}^-\right|^2 = \frac{T_c R_s \left|\tilde{c}^+\right|^4}{\left|\tilde{b}^+\right|^2}$$

The ratio of return to forward wave ring power in this case is defined as β_R,

$$\beta_R' = \frac{|\tilde{c}^-|^2}{|\tilde{c}^+|^2} = \frac{T_c R_s |\tilde{c}^+|^2}{|b^+|^2} = \frac{T_c T_R R_s}{R_R} \frac{P_{osc}}{P_0}$$

$$\beta_R' = \frac{T_c T_R R_s}{R_R} \frac{P_{osc}}{P_0} \tag{15}$$

Note the comparison of β_R and β_R' equations 8 and 15 for the two regimes. The ratio of return to forward power for the MO in this case can be written as,

$$\beta_L' = \frac{|\tilde{b}^-|^2}{|\tilde{b}^+|^2} = \frac{T_c^2 R_s}{} |\tilde{c}^+|^4$$

$$= \frac{T_c^2 T_R^2}{R_R^2} R_s \left(\frac{P_{osc}}{P_0}\right)^2$$

$$= \frac{T_c^2 R_s}{\delta_\ell^4} \tag{16}$$

Note the comparison of β_L and β_L' (eq. (10) and (12))for the two regimes. In particular,

$$\beta_L' = \frac{R_R^2}{T_c} \beta_L^2 \tag{17}$$

It appears that if adequate suppression can be achieved with a suppression mirror i.e. β_L<.01 for example; then injection will provide even better suppression for most cases of interest without the use of a retro-reflector.

i.e. let

$$R_R = 0.5 \quad \text{(outcoupling of ring)}$$

$$T_c = 0.1 \quad \text{(backward wave outcoupling)}$$

then,

$$\beta_L' = 2.5\ \beta_L^2$$

and if $\beta_L = .01$

$$\beta_L' = 2.5 \times 10^{-4}.$$

Note that all of the previous results are only valid when β_L and β_L' are small compared to unity.

The analysis of return wave suppression with a combination of injection control and a retro-reflector can be performed via equations (13) and (14). This is an important endeavor which has not been attempted as yet. It is apparent that the combined use of injection control and retro-reflector places some constraints on the phasing of the retro-reflected beam and the injected beam. A separate control of mirror M_9 in the ring resonator layout may be required in order to improve on the return wave suppression achievable by injection control alone.

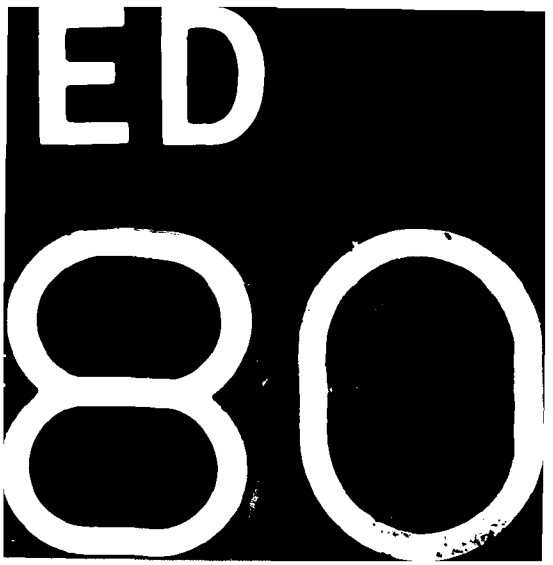
ED
80